



UNIVERSITEIT•STELLENBOSCH•UNIVERSITY
jou kennisvenoot • your knowledge partner

Scenarios for a South African Peaking CSP System in the Short-Term

Cebo Silinga

A Master's project presented in partial fulfilment of the requirements for
the degree of

Master of Engineering at University of Stellenbosch

Supervisor: Mr Paul Gauché

April 2014



Departement Meganiese en Megatroniese Ingenieurswese
Department of Mechanical and Mechatronic Engineering



Declaration

By submitting this thesis electronically, I declare that the entirety of the work contained therein is my own, original work, that I am the sole author thereof (save to the extent explicitly otherwise stated), that reproduction and publication thereof by Stellenbosch University will not infringe any third party rights and that I have not previously in its entirety or in part submitted it for obtaining any qualification.

December 2013

ABSTRACT

South African electricity demand is characterized by morning and evening peak periods, occurring between 07:00–09:00 and 18:00–20:00. In order to meet the peak period electricity demand, flexible systems with quick start-up times are needed. During the peak periods, any technology that is able to supply electricity at competitive prices is valuable. Currently, South Africa utilises Open Cycle Gas Turbine (OCGT) plants to supply peak electricity. There is 2 426 MW of installed OCGT capacity, all of which are run on diesel. The current plans are to increase the installed capacity of the OCGT plants relative to increasing electricity demand.

The South African Integrated Resource Plan (IRP) is a policy document that by law allocates the energy resources that will be built to meet the country's future electricity needs. The IRP indicates the electricity generation technology types that will be built from 2010 to 2030. It states that most of the future peak load will be met by OCGT plants and represents an allocation of 4 930 MW. Further, the IRP allocates 1 200 MW of capacity to Concentrating Solar Power (CSP) as renewable but does not identify CSP systems as a potential peaking solution. This allocation represents less than 2 % of total capacity in 2030. Analyses suggests that OCGTs generate electricity at a cost in excess of 5.00¹ ZAR/kWh. This cost is significantly above current costs of CSP with thermal energy storage to service the evening peaks, which are in the order of 1.82 ZAR/kWh.

This project investigates the feasibility of utilizing CSP plants as peaking plants in the short- to medium-term based on a proposition that under certain scenarios, a fleet of unsubsidized CSP peaking plants could drop the Levelised Cost of Electricity (LCOE) of the current IRP. This is done by modelling a system of contemporary CSP central receiver plants, obtaining the LCOE and comparing it with the OCGT system LCOE. The Gemasolar plant in Spain, which can operate continuously using thermal energy storage, was used as a reference plant in order to obtain operating parameters.

Two alternate scenarios show a lower LCOE for providing peak power. The first scenario is the utilisation of CSP with grid energy. The national grid is used for the energy demand gap during the operation of the CSP system. This is demonstrated by charging the hot salt tank (thermal energy storage) during periods of inadequate solar resource. The LCOE for this system is 1.89 ZAR/kWh for the CSP system energy supply. The LCOE of the combined system—CSP and grid energy—increases from 1.89 ZAR/kWh to 3.00 ZAR/kWh.

¹ Conversion rates are calculated with R 8.00 per US \$. South African Rand = ZAR

The most promising scenario—second scenario is a combined distributed CSP system with diesel powered OCGT system as backup. The LCOE for this system is 2.78 ZAR/kWh or a drop of 45 % in OCGT LCOE.

The proposal is to build CSP plants in phases, in line with electricity demand projections, and to gradually spread the CSP system along the transmission line from both ends to ensure optimal usage of the solar resource.

OPSOMMING

Suid-Afrika se elektrisiteitsaanvraag word gekenmerk deur oggend en aand piektye: tussen 7:00 en 9:00, en tussen 18:00 en 20:00. Om aan die piektyd se aanvraag te voldoen moet aanpasbare stelsels met vinnige begintye daargestel word. Gedurende die piektye is enige tegnologie wat elektrisiteit teen mededingende pryse kan verskaf baie waardevol. Tans gebruik Suid-Afrika Oop Siklus Gasturbine (Open Cycle Gas Turbine (OCGT)) aanlegte om elektrisiteit te voorsien gedurende piektye. Daar is tans 2 426 MW geïnstalleerde OCGT kapasiteit wat alles d.m.v. diesel aangedryf word. Huidige planne is om die geïnstalleerde kapasiteit van die OCGT aanlegte te verhoog relatief tot die groeiende elektrisiteitsaanvraag.

Die Suid-Afrikaanse Geïntegreerde Hulpbronplan (Integrated Resource Plan (IRP)) is 'n beleidsdokument wat volgens wet energie hulpbronne toewys om gebou te word om sodoende aan die toekomstige Suid-Afrikaanse elektrisiteitsbehoefte te voldoen. Die huidige IRP toon die elektrisiteitsopwekking tegnologie tipes wat tussen 2010 en 2030 gebou gaan word. Die dokument stel dat die OCGT aanlegte die meeste van die toekomstige piektydaanvraag sal kan dra en verteenwoordig 'n toewysing van 4 930 MW. Verder hiertoe sien die IRP nie Gekonsentreerde Sonkrag (Concentrating Solar Power (CSP)) as 'n potensiële piektyd-oplossing nie en allokeer 1 200 MW aan die kapasiteit as hernubaar. Hierdie verteenwoordig minder as 2 % van die totale kapasiteit in 2030. Analise voer aan dat OCGTs elektrisiteit opwek teen 'n koste wat 5.00 ZAR/kWh oorskry; beduidend bo die huidige kostes van CSP met termiese energieberging om die aand piektye te diens wat nader is aan 1.82 ZAR/kWh.

Hierdie projek ondersoek die lewensvatbaarheid daarvan om CSP aanlegte as piektydvoorsieners te gebruik in die kort tot medium termyn gebaseer op 'n voorstel dat daar met sekere scenarios, 'n vloot van ongesubsideerde CSP piekaanlegte kan die Levelised Cost of Electricity (LCOE) van die huidige IRP verminder. 'n Stelsel is gemodelleer wat die hedendaagse CSP sentrale ontvanger aanlegte, en die LCOE te kry en te vergelyk met die OCGT stelsel se LCOE. Die Gemasolar aanleg in Spanje, wat ononderbroke kan werk met termiese energieberging, is gebruik as verwysingsaanleg om werkbare parameters te verkry.

Twee alternatiewe scenarios toon 'n laer LCOE om piekkrag te voorsien. Die eerste scenario is om CSP saam met die elektrisiteitsvoorsiener te gebruik. Die nasionale voorsiener word gebruik vir die gaping in energieaanvraag met die gebruik van die CSP stelsel. Dit word gedoen deur 'n warm souttenk (termiese energieberging) te laai tydens tye van 'n onvoelende sonhulpbron. Die LCOE vir hierdie stelsel is 1.89 ZAR/kWh vir die CSP stelsel se energievoorsiening. Die LCOE vir die gekombineerde stelsel (CSP en roosterenergie) is 3.00 ZAR/kWh.

Die mees belowende is 'n gekombineerde verdeelde CSP stelsel met 'n diesel-aangedrewe OCGT stelsel as steundiens. Die LCOE vir hierdie stelsel is 2.78 ZAR/kWh of 'n daling van 45 % in die OCGT LCOE.

Die voorstel is om aanlegte in fases te bou, in lyn met die elektrisiteitsaanvraag se vooruitskattings, en om geleidelik die CSP stelsel te versprei al langs die kraglyn van beide kante om optimale gebruik van die sonkragbron te verseker.

ACKNOWLEDGEMENTS

First, I would like to thank my supervisor Mr Paul Gauché for his support and valuable input. His advice and encouragement to pursue this study and the assistance throughout the entire degree is much appreciated.

I would also like to thank Centre for the Renewable and Sustainable Energy Studies (CRSES) and the Solar Thermal Research Group (STERG) at Stellenbosch University for funding and support. The advice and support from Prof Wikus van Niekerk (CRSES). STERG researcher, Christina Auret is thanked for suggesting scenario 3 which is the scenario showing the ideal solution.

TABLE OF CONTENTS

| | |
|--|------|
| ABSTRACT | i |
| OPSOMMING | iii |
| ACKNOWLEDGEMENTS..... | v |
| TABLE OF CONTENTS | vi |
| LIST OF FIGURES..... | x |
| LIST OF TABLES..... | xii |
| ACRONYMS | xiii |
| NOMENCLATURE | xiv |
| 1 Introduction | 1 |
| 1.1 Objective..... | 2 |
| 1.2 Methodology | 2 |
| 1.3 Scope of Report | 3 |
| 1.4 Motivation..... | 3 |
| 1.5 Chapter Overview | 4 |
| 2 Literature Survey..... | 5 |
| 2.1 South African Energy Industry Overview | 5 |
| 2.1.1 Integrated Resource Plan..... | 6 |
| 2.1.2 Renewable Energy Independent Power Producer Procurement Programme | 7 |
| 2.1.3 Infrastructure Analysis (Grid status review) | 8 |
| 2.2 Peaking Power Plants Overview | 8 |
| 2.2.1 Open Cycle Gas Turbine (OCGT) | 8 |
| 2.2.2 Pumped Storage..... | 9 |
| 2.3 General Developments Overview | 10 |

| | | |
|-------|---|----|
| 2.3.1 | Astronomy Geographic Advantage Act..... | 10 |
| 2.3.2 | Hydraulic Fracturing | 11 |
| 2.4 | Previous Studies on CSP Dispatchability | 11 |
| 2.5 | CSP Systems Overview | 14 |
| 2.5.1 | Stirling Dish System | 15 |
| 2.5.2 | Linear Fresnel System | 16 |
| 2.5.3 | Parabolic Trough System | 17 |
| 2.5.4 | Central Receiver (Tower) System | 18 |
| 2.5.5 | Comparison: CSP Tower vs CSP Trough..... | 19 |
| 2.6 | Conclusion | 19 |
| 3 | Supply and Demand for Peaking..... | 20 |
| 3.1 | Load Demand for Peaking..... | 20 |
| 3.2 | CSP Central Receiver Plant..... | 22 |
| 3.2.1 | Gemasolar Power Plant | 22 |
| 3.2.2 | Thermodynamic Cycle | 24 |
| 3.3 | Open Cycle Gas Turbine (OCGT) | 24 |
| 3.4 | Levelised Costs of Electricity..... | 26 |
| 3.4.1 | Levelised Costs of Electricity – OCGT..... | 27 |
| 3.4.2 | Levelised Costs of Electricity – CSP..... | 27 |
| 3.5 | Conclusion | 27 |
| 4 | Technical Model Development | 28 |
| 4.1 | CSP Plant Model Development | 28 |
| 4.1.1 | Heliostat Field Background | 28 |
| 4.1.2 | Heliostat Optical Losses..... | 29 |
| 4.1.3 | Heliostat Field Losses | 29 |

| | | |
|--------|---|----|
| 4.1.4 | Receiver Background..... | 32 |
| 4.1.5 | Receiver Geometry | 33 |
| 4.1.6 | Receiver Energy Balance..... | 34 |
| 4.1.7 | Thermal Storage System Operating Parameters..... | 35 |
| 4.1.8 | Power Block..... | 35 |
| 4.1.9 | Parasitic Power | 36 |
| 4.1.10 | Power Plant Scaling | 36 |
| 4.2 | OCGT Plant Model..... | 38 |
| 4.3 | Conclusion | 38 |
| 5 | Scenario Modelling..... | 39 |
| 5.1 | Business as Usual Scenario: OCGT Energy Supply..... | 39 |
| 5.1.1 | OCGT Analysis of LCOE..... | 40 |
| 5.1.2 | Fuel Sensitivity Study..... | 41 |
| 5.2 | CSP System Description | 42 |
| 5.3 | Scenario 2 – CSP + Grid Electricity Thermal Energy Supply | 43 |
| 5.3.1 | CSP System LCOE Study | 44 |
| 5.3.2 | Grid Energy Supply Analysis | 47 |
| 5.3.3 | Eskom Flexi Rates | 48 |
| 5.3.4 | National Load Demand Increase | 49 |
| 5.3.5 | Grid Electricity Purchase Guarantee | 49 |
| 5.4 | Scenario 3 – Combined CSP System and OCGT System..... | 51 |
| 5.4.1 | LCOE CSP System..... | 52 |
| 5.4.2 | LCOE OCGT System | 53 |
| 5.4.3 | OCGT LCOE Fuel Sensitivity Analysis..... | 53 |
| 5.4.4 | Combined LCOE..... | 53 |

| | | |
|-----|--|----|
| 5.5 | Conclusion | 54 |
| 6 | Implementation Proposal..... | 55 |
| 6.1 | Implementation Plan Costs Analysis | 55 |
| 6.2 | Power Plants Locations..... | 57 |
| 6.3 | GIS Study of Land Availability | 57 |
| 6.4 | Conclusion | 59 |
| 7 | Conclusions and Further Work..... | 60 |
| 8 | References..... | 61 |
| | APPENDIX A – ZENITH ANGLE CALCULATION | 67 |
| | APPENDIX B – POWER PLANT SCALING..... | 69 |
| | APPENDIX C – CURTAILMENT | 71 |
| | APPENDIX D – COMPARISON OF ACTUAL DNI VS PREDICTED DNI | 72 |
| | APPENDIX E – POWER PLANTS LOCATIONS | 73 |

LIST OF FIGURES

| | |
|---|----|
| Figure 1.4.1: South African solar resource and proposed CSP sites | 4 |
| Figure 2.3.1: RFI reserve and shalegas exploration | 11 |
| Figure 2.4.1: Energy production by hour of day | 12 |
| Figure 2.4.2: Sample of dispatch of a CSP plant with six hours of TES | 13 |
| Figure 2.4.3: Summer results (only three models with baseline storage | 14 |
| Figure 2.4.4: Winter results (only the three models with baseline storage | 14 |
| Figure 2.5.1 Stirling dish system configuration | 15 |
| Figure 2.5.2: Linear Fresnel system configuration | 16 |
| Figure 2.5.3: Parabolic trough system configuration | 17 |
| Figure 2.5.4: Central receiver system configuration..... | 18 |
| Figure 3.1.1: Peak load definition schematic illustration | 20 |
| Figure 3.1.2: January/June load demand | 21 |
| Figure 3.2.1: CSP plant configuration..... | 22 |
| Figure 3.2.2: Gemasolar CSP power plant | 23 |
| Figure 3.2.3: T-s diagram of saturated and superheated steam Rankine cycle.. | 24 |
| Figure 3.3.1: Open Cycle Gas Turbine (OCGT) configuration | 25 |
| Figure 3.3.2: T-s diagram of Brayton cycle | 25 |
| Figure 4.1.1: Heliostat optics | 29 |
| Figure 4.1.2: Cosine effect on the heliostat spectrum | 30 |
| Figure 4.1.3: Blocking and shading from the solar field | 31 |
| Figure 4.1.4: Representation of optical losses curve fit..... | 32 |
| Figure 4.1.5: External receiver efficiency curve | 33 |
| Figure 4.1.6: External receiver energy balance | 34 |
| Figure 4.1.7: CSP system components scaling | 38 |

| | |
|---|----|
| Figure 5.1.1: Lifetime costs of OCGT system | 41 |
| Figure 5.1.2: OCGT system LCOE fuel sensitivity analysis | 42 |
| Figure 5.2.1: Annual average sum of DNI from 10 selected sites | 43 |
| Figure 5.3.1: CSP system operation configuration..... | 44 |
| Figure 5.3.2: Storage charge level and energy curtailment – random site | 46 |
| Figure 5.3.3: TES grid energy purchase | 47 |
| Figure 5.3.4: National electricity demand load profile increase | 49 |
| Figure 5.3.5: Grid electricity purchase fulfilment analysis. | 50 |
| Figure 5.3.6: CSP system + grid electricity fulfilment analysis | 50 |
| Figure 5.4.1: CSP system operation configuration..... | 52 |
| Figure 5.4.2: Combined LCOE of OCGT and CSP | 54 |
| Figure 6.1.1: Implementation proposal LCOE sensitivity analysis..... | 55 |
| Figure 6.1.2: Implementation Proposal fulfilment coefficient analysis | 56 |
| Figure 6.1.3: Implementation proposal curtailment coefficient analysis..... | 57 |
| Figure 6.3.1: Land availability along the proposed sites (short-term) | 59 |
| Figure A.1: Sun angles relative to the heliostat spectrum | 67 |
| Figure B.1: CSP primary components | 69 |
| Figure B.2: Solar field and tower scaling | 70 |
| Figure B.3: TES scaling..... | 70 |
| Figure C.1: Storage charge level and energy curtailment – total system | 71 |
| Figure D.1: Actual DNI vs predicted DNI | 72 |
| Figure E.1: Land availability along the proposed sites (long-term)..... | 73 |

LIST OF TABLES

| | |
|--|----|
| Table 2.1: IPP projects for the REIPPPP | 7 |
| Table 2.2: South African OCGT capacity | 9 |
| Table 2.3: Hydroelectric power stations in South Africa | 9 |
| Table 2.4: Commercially available two tank TES | 19 |
| Table 3.1: Gemasolar power plant specifications | 23 |
| Table 4.1: Chambadal-Novikov efficiency and actual efficiency comparison | 36 |
| Table 5.1: OCGT costs breakdown | 40 |
| Table 5.2: OCGT capital and O&M costs | 41 |
| Table 5.3: CSP system configuration | 42 |
| Table 5.4: CSP system capital and O&M costs | 45 |
| Table 5.5: CSP delivered peak energy | 45 |
| Table 5.6: CSP system LCOE results | 45 |
| Table 5.7: TES thermal losses efficiency | 48 |
| Table 5.8: Eskom RURAFLEX tariffs | 48 |
| Table 5.9: Grid energy purchase results | 50 |
| Table 5.10: Combined CSP and grid energy results | 51 |
| Table 5.11: CSP system and OCGT proposed capacity | 51 |
| Table 5.12: CSP energy delivered and the LCOE | 52 |
| Table 5.13: OCGT energy delivered and the LCOE | 53 |
| Table 5.14: CSP combined with OCGT LCOE | 54 |

ACRONYMS

| | |
|---------|--|
| CES | Conventional Energy Systems |
| CRSES | Centre for Renewable and Sustainable Energy Studies |
| CSP | Concentrating Solar Power |
| DNI | Direct Normal Irradiation |
| DoE | Department of Energy |
| DSG | Direct Steam Generation |
| DST | Department of Science and Technology |
| GIS | Geographic Information Systems |
| HTF | Heat Transfer Fluid |
| IEP | Integrated Energy Plan |
| IPP | Independent Power Producer |
| IRP | Integrated Resource Plan |
| LCOE | Levelised Costs of Energy |
| NERSA | National Energy Regulator of South Africa |
| NREL | National Renewable Energy Laboratory |
| OCGT | Open Cycle Gas Turbine |
| O&M | Operation and management costs |
| RE | Renewable Energy Systems |
| RFI | Radio Frequency Interference |
| REIPPPP | Renewable Energy Independent Power Procurement Power Program |
| SA | South Africa |
| TES | Thermal Energy Storage |
| ZAR | South African Rand |

NOMENCLATURE

| | |
|--------------------|--------------------------------------|
| A_a | aperture area of the solar field |
| A_i | receiver emitting area |
| E_t | electricity generation in the year t |
| F_i | receiver view factor |
| F_t | fuel expenditures in the year t |
| h | heat transfer coefficient receiver |
| I_t | investment expenditure in the year |
| M_t | O&M expenditures in the year t |
| n | life of the system |
| $\dot{Q}_{in/out}$ | heat flow receiver |
| r | discount rate |
| T_a | ambient temperature |
| T_H | receiver outlet temperature |
| $\bar{T}_{r/ri}$ | mean temperature receiver |
| \dot{W} | work done |
| η_{th} | thermal efficiency |
| $\eta_{optical}$ | solar field optical efficiency |
| ε_r | receiver emissivity |
| σ | Stefan-Boltzmann constant |
| α | receiver absorptivity |
| θ_Z | Zenith angle |
| φ | Latitude |
| δ | Declination angle |
| ω | hour angle |

1 Introduction

The South African electricity industry is faced with the challenge of generating and supplying adequate electricity to meet demand. What have become characteristic of the South African electricity industry are the stretched reserve margin and the inevitable increasing electricity prices. Over the past decade South Africa (SA) experienced periods of black-outs due to lack of sufficient electricity capacity availability. Since then the national utility company, Eskom, has been faced with the challenge of having an adequate reserve margin. At the end of Summer 2013, Eskom was operating with the reserve margin of 1 % (M&G 2013a). This reserve margin is lower than the industry best practice of about 15% (Eskom 2012a). The reserve margin is stretched during peak periods when there is a sudden increase in electricity demand.

The morning peak period typically occurs between 07:00 – 10:00. The evening peak typically occurs between 18:00 – 20:00 (Eskom 2012a). In order to meet the peak period electricity demand, flexible energy systems with quick start-up times are needed. During the peak periods, any energy system that is able to supply energy at competitive prices is valuable.

During the tariff increase period of April 2010 – March 2013, electricity prices increased at an average rate of 25 % (Creamer 2013). Eskom applied for a tariff increase of 16 % to take effect during 2013 – 2017. The National Energy Regulator of South Africa (Nersa) rejected that increase but approved a tariff increase of 8 % (M&G 2013b).

Perhaps, the most important policy document to emerge in the South African electricity industry is the Integrated Resource Plan (DoE 2011), hereafter referred to as the IRP. The IRP details the types of energy systems that will be built over the period between 2010 and 2030. This important legal document outlines the short- and long-term plans for the South African electricity industry (DoE 2011). The IRP is intended to be a living document with periodic updates.

The Integrated Energy Plan (IEP) is a new, overarching long-term plan for the energy sector. As compared to the IRP, which is the electricity plan, the IEP will cover the full energy spectrum; electricity, liquid fuel and gas (DoE 2013). The next revision of the IRP will come up under the electricity section of the IEP. Currently, the IEP is in the public-consultation phase and the Department of Energy (DoE) plans to publish it during the course of 2014 (DoE 2013).

The IRP allocates capacity to all electricity generating technologies that will be used to meet baseload, intermediate load and peak load demands. The IRP indicates how the peak load will be met and which electricity systems will be built in order to meet them.

In the IRP, the Open Cycle Gas Turbine (OCGT) electricity generating systems are identified as a primary technology that will be used as peaking power plants (DoE 2011). These power plants offer some advantages due to their low capital costs, quick installation period and ease of operation. The most significant drawback to operating these power plants is the high running costs due to high fuel cost (Brinckerhoff 2008).

The IRP identifies Concentrating Solar Power (CSP) technology as one of the renewable energy systems that will contribute to the electricity supply (DoE 2011). It does not identify CSP as a potential peaking solution. The allocation of CSP is small, but a number of advantages suggest significant potential to increase the allocation in the system, primarily due to dispatchability.

A value proposition for CSP in the South African context has been proposed by Gauché et al. (2012). The authors suggest that CSP is a good match for the country in the long term provided action is taken soon. They recognise the dilemma due to the barriers of cost and uncertainty. The high marginal cost of peaking electricity presents an opportunity to address this barrier. Thus, the following question is posed: Can an alternative peaking system that includes CSP be more cost-effective than the existing planned peaking system using only currently available infrastructure and CSP technology?

1.1 Objective

The main research aims of this study are:

- To investigate the financial feasibility and performance viability of utilising CSP for electricity in South Africa in the short-term.
- To determine measures that guarantee the delivery of electricity from the peaking system that is primarily CSP based.

This objective is done by modelling a contemporary system of CSP plants, obtaining the system Levelised Cost of Electricity (LCOE) and comparing it with the LCOE of an OCGT system. The criteria used to determine the feasibility of CSP in this role is the LCOE and the guarantee of electricity to the grid.

1.2 Methodology

The proposed CSP system² is comprised of distributed CSP plants situated along the high-voltage, high-capacity line that runs towards Cape Town from Gauteng

² The word “system” has various meanings to participants in the electricity sector. As this study deals with many of these meanings, some terminology needs to be clarified.

province (see Figure 1.4.1). The idea here is to make the system more feasible in the short-term by being in close proximity to the existing transmission system, thus requiring less infrastructure investment. The proposed CSP system capacity is to be optimized for meeting demand with lowest cost.

This is done by the following:

- Conducting a literature study – this considers the energy resources, electricity technologies and the relevant electricity policy.
- Defining the operating parameters of CSP technical model, OCGT technical model and the financial model of CSP and OCGT system.
- Proposing scenarios for a peaking CSP system.
- Optimizing the CSP model to seek the lowest cost of electricity and a guarantee of supply.
- Conducting an analysis of results and proposing a way forward, including an implementation proposal.

Figure 1.4.1 indicates the proposed sites, the solar resource (direct normal irradiation - DNI) and the transmission infrastructure. Ten distributed locations, approximately equally spaced, are coincident with the high capacity line and in a band of sufficient to good solar resource. These sites will be referred to as the “proposed sites”.

1.3 Scope of Report

There are various electricity systems that are utilized to meet the peak electricity demand. Pumped hydro storage is one that is utilised in SA with costs benefits, but it is not considered for this study. In this study only the peaking OCGT systems are considered as reference peak electricity systems: the electricity generation costs of the peaking CSP system are compared to the electricity generation costs of the peaking OCGT system.

1.4 Motivation

This project is about the peaking CSP system for near-term solutions, which if successful could have meaningful implications. SA may be facing more electricity problems in future, particularly in the supply of peak electricity. The existing planned peaking solution is expensive. This project aims to evaluate an idea that, if successful, can have a significant impact on the cost and security of electricity supply. It could also be the catalyst to test the broader CSP value as it presents a potential first step for applying renewables from a purely economic point of view.

Reference to “CSP system”, “OCGT system” or “peaking system” amongst others generally refers to a system of plants.

2 Literature Survey

This chapter provides a review of the South African electricity industry by reviewing the resources, technologies and policies. This will be done by giving a review of the current structure of the electricity industry. In order to understand the dynamics of the electricity industry in general, this section will be followed by a review of the different energy industry policies that are linked to the development of the renewable energy systems. The last part of the chapter will give a review of the CSP technologies by presenting the technical description and current status of development.

2.1 South African Energy Industry Overview

The South African electricity industry is characterised by the single, vertically integrated state utility, Eskom. Eskom is the South African government entity that is responsible for generation, transmission and distribution of electricity. In 2012, Eskom generated 98 % of the South African energy demand (Eskom 2012a).

Until the recent development of the Renewable Energy Independent Power Producer Procurement Programme (REIPPPP), the implementation of the IRP, Eskom primarily decided what electricity systems to build. Eskom is currently constructing coal power plants to increase the installed capacity. The build programme is comprised of Medupi, Kusile coal plant. In addition to that is the Ingula pumped storage (Eskom 2012a). The plant includes a 100 MW wind farm and a planned 100 MW CSP plant (Eskom 2012a). The total capacity in the current build program and planned plants is 11 152 MW, with 9 617 MW being from coal plants.

The South African electricity industry is dependent on coal, which is a finite resource. This reliance is based on the cheap coal reserves estimations, which predicted that SA has abundant coal reserves. However, over the years the prediction of these coal reserves has been reduced. Between the years 2003, 2004 and 2005 the Department of Minerals and Energy reduced the South African coal reserves estimations from 50, 31 and 26 Giga tonnes respectively. In 2008, the BP Statistical Review of World Energy reduced the South African coal reserve estimates by 18 Giga tonnes - from the previous year estimates of 48 Giga tonnes to 30 Giga tonnes (Hartnady 2010).

The Hubbert (1956) method of predicting peak period has been proven reliable at predicting peak and production of oil in mature regions and depleted regions. The Hubbert (1956) method uses the historical production data fitted to a normal distribution curve. If sufficient production has occurred, at a point where the rate of production starts to decline, peak period and ultimate production are predicted with higher accuracy than the geological estimates predict (Hubbert 1956).

Patzek & Croft (2010) use a multi-Hubbert cycle analysis to determine the global coal production. Rutledge (2011) developed and uses a model that uses the cumulative normal model for all the coal regions around the world. Hartnady (2010) developed a similar method to estimate the African reserves by using the Rutledge updated data.

The study by Rutledge (2011) indicates that South African coal will reach 90 % cumulative extraction by 2048 at 18.6 Giga tonnes. Hartnady (2010) predicts that South African coal peak production year will be in 2020 at 284 Mega tonnes and will reach 90 % cumulative extraction at 23 Giga tonnes. Hartnady (2010) revised the previous coal peak production year to 2013 at 254.3 Mega tonnes. Patzek & Croft (2010) predict that the South African coal production has peaked already in 2007 and the 90 % cumulative extraction is predicted to be 17.15 Giga tonnes.

2.1.1 Integrated Resource Plan

The IRP 2010 – 2030 is a policy document for the South African electricity sector. It is legal document that states what electricity systems will be built in the country. The IRP was first crafted in 2010 and it allocates capacity to various electricity systems that will be built up until 2030. The IRP is a significant policy document for the South African electricity industry because it provides a road map for the electricity industry. One of the key achievements of the IRP is that it acknowledges the need to diversify the electricity supply and adopt more sustainable electricity systems that emit less greenhouse gasses.

The IRP only allocates 6 GW of coal capacity to be built after the current build programme by Eskom (DoE 2011). This allocation considers the greenhouse gas emissions challenge, especially when looking at the fact that it strives to reduce the greenhouse gas emitting systems from the energy systems capacity. The IRP further allocates the amount of capacity to the renewable energy systems: 8.4 GW PV, 8.4 GW wind, 2.6 GW imported hydro and 1.2 GW of CSP capacity (DoE 2011).

The IEP is a new overarching long-term plan for the energy sector. As compared to the IRP, which is the electricity plan, the IEP will cover the full energy spectrum; electricity, liquid fuel and gas (DoE 2013). The next revision of the IRP will come up under the electricity section of the IEP. Currently, the IEP is in the public-consultation phase and the DoE plans to publish it in 2014. The draft IEP indicates that solar resource in SA has an electricity generation potential of 60 GW. It also states the need to invest in transmission infrastructure from the areas of high solar resource to the main electricity demand centres (DoE 2013).

2.1.2 Renewable Energy Independent Power Producer Procurement Programme

The REIPPPP is a DoE programme that implements the renewable energy allocations of the IRP in SA. The REIPPPP is responsible for allocating capacity for various renewable energy technologies. The Independent Power Producers (IPP) submit bids for the systems that they intend to build depending on the capacity allocation (REIPPPP 2013).

The REIPPPP has allocated a capacity of 3 725 MW for all renewable energy technologies that are in the IRP to be implemented now. This capacity is divided among all these technologies based on the IRP allocation ratio. CSP had an allocation of 200 MW. During the first bidding round, 150 MW of new CSP plants were awarded. The second bidding round awarded the remaining 50 MW of CSP. The tariffs for the first and second bidding rounds were capped at 2 850 R/MWh. After the second round, all the allocated CSP capacity had been taken up by the IPPs (REIPPPP 2013).

During round three, a further 200 MW capacity was allocated for CSP. The tariffs were also changed for the CSP during the third round: 1 650 ZAR/MWh for off-peak and 3 960 ZAR/MWh for peak period. The third bidding round awarded the allocated 200 MW of CSP (REIPPPP 2013).

Table 2.1 shows the CSP projects of the IPPs that are developed under the REIPPPP. These are projects from the first and second rounds that were based on fixed tariffs with no emphasis on energy storage. The third round tariff structure will allow the developers to invest in thermal energy storage (TES) in order to supply during peak period.

Table 2.1: IPP projects for the REIPPPP (REIPPPP 2013)

| Name of the plant | Bidding Round | Type of plant | Capacity (MW) | TES (hours) |
|--------------------------|----------------------|----------------------|----------------------|--------------------|
| KaXu Solar One | 1 | Parabolic Trough | 100 | 3 |
| KHI Solar | 1 | Central Receiver | 50 | 2 |
| Bokpoort | 2 | Parabolic Trough | 50 | 9 |
| Xina Solar | 3 | Parabolic Trough | 100 | 5 |
| Ilanga CSP 1 | 3 | Parabolic Trough | 100 | 4.5 |

2.1.3 Infrastructure Analysis (Grid status review)

The infrastructure analysis that is considered in this study is the connection capacity of the transmission network. The current grid was developed to service the centralized power plants – typically coal plants that are situated in the northern parts of the country close to the coal mines (Eskom 2010b). The renewable energy resource is available in various parts of the country where the electricity grid infrastructure is not adequate. This grid capacity challenge makes it crucial to study the electricity grid ability to accommodate new renewable energy systems.

Eskom acknowledged this need and conducted a study to look at the short-term status of the electricity grid connection capacity. Their study identified the Northern Cape, Eastern Cape and Western Cape as the zones with the most potential for renewable energy projects, hence only considering them for the analysis (Eskom 2010b). The initial study by Eskom shows that the current transmission infrastructure feed-in capabilities are not sufficient to accommodate the renewable energy systems in the IRP horizon. Eskom is currently undertaking an electricity grid connection capacity upgrade, which would allow the developers to feed-in electricity to the grid at lower costs (Eskom 2010b). However, this infrastructure upgrade is a long-term project.

Eskom concludes that there is currently 6 700 MW connection capacity from all three provinces (Eskom 2010b) with the East Zone having 1 042 MW, the West Zone 2 988 MW and the North Zone 129 MW. What this analysis shows is that, in the short-term, there is available feed-in capacity for the renewable energy developers to utilize; however, in the long-term - IRP horizon, the current Eskom grid upgrade programme is crucial in order to create adequate electricity grid capacity.

2.2 Peaking Power Plants Overview

This section will give an overview of the current peaking electricity systems that are utilized in SA. This will be done by considering the OCGT electricity systems and the Pumped Storage electricity system.

2.2.1 Open Cycle Gas Turbine (OCGT)

Currently, OCGT systems perform a significant role within the South African electricity industry, supplying peak period electricity. Eskom owns and operates the OCGT power stations.

Eskom has a capacity of 2 426 MW of OCGT. Table 2.2 indicates the names and locations of the OCGT stations. The Ankerlig and Gourikwa power stations were built just before the country experienced power cuts in 2008.

The decision to build these stations was based on Eskom's realization that the reserve margin was strained and power cuts were eminent (Eskom 2009). There were various reasons that drove Eskom's decision to build these two stations, but it was mainly because the stations could be constructed in a short period of time (Eskom 2009).

Table 2.2: South African OCGT capacity

| Power Plant | No of units | Installed Capacity | Commission Date |
|-------------------------|----------------------|---------------------------|------------------------|
| Ankerlig (Atlantis, WC) | 4 * 149.2; 5 * 148.2 | 1 338 MW | 2007 |
| Gourikwa (Mossel Bay) | 5 * 149.2 | 746 MW | 2007 |
| Acacia (Cape Town) | 3 * 57 | 171 MW | No information |
| Port Rex (East London) | 3 * 57 | 171 MW | No information |

The IRP allocates 4 930 MW capacity to the OCGT. This is based on the OCGT systems' operational flexibility in general and their ability to be quickly synchronised with the grid. Currently, OCGT systems in SA are run on diesel fuel.

2.2.2 Pumped Storage

Table 2.3: Hydroelectric power stations in South Africa

| Name of system | Value | Unit | Type of system |
|-----------------------|--------------|-------------|-------------------------------------|
| Drakensberg | 1 000 | MW | Pumped storage |
| Palmiet | 400 | MW | Pumped storage |
| First falls | 6.4 | MW | Run-off-river |
| Second falls | 11 | MW | Run-off-river |
| Colley Wobbles | 42 | MW | Run-off-river |
| Ncora | 2.4 | MW | Run-off-river |
| Gariep | 360 | MW | Conventional reservoir |
| Vanderkloof | 240 | MW | Conventional reservoir |
| Ingula | 1 332 | MW | Pumped storage (under construction) |

Hydroelectricity has the benefit of being able to provide baseload as well as peak load.

A pumped storage system stores energy during off-peak periods and delivers that energy during peak periods. Eskom, in collaboration with other stake holders, owns two conventional reservoir stations, two run-off-river stations and two pumped storage stations (Eskom 2012a).

Table 2.3 shows the list of current hydro power stations in SA. What this table makes clear is that hydro power plays a small part in the South African energy industry. The combined listed stations generated 2 % of the total energy delivered in 2012 (Eskom 2012a). This low percentage is based on the fact that SA is a water scarce country, and the viable pumped hydro sites are limited.

Pumped hydro is the most economical peaking energy system with estimated capital costs of 7 913 ZAR/kW (DoE 2011). Due to South Africa's environment and arid climate, the potential for pumped hydro is limited. The IRP predicts that about 3 349 MW of capacity will be sourced from new hydro (DoE 2011); however, all that hydro will be import hydro. There are countries with hydro potential that are adjacent to South Africa, but climatic uncertainty and political instability in those countries are a concern. While hydro is a well proven, cost effective energy storage medium, especially when utilized as pumped hydro storage, SA does not have adequate water supply needed for such a system. Moreover, the proven sites for the hydro pumped storage are limited (DoE 2011).

2.3 General Developments Overview

This section gives an overview of the developments and policies that are not necessarily in the electricity industry but need to be considered in the development of renewable energy systems.

2.3.1 Astronomy Geographic Advantage Act

The Astronomy Geographic Advantage Act (AGAC) of 2007 was developed to protect the area that is identified for the Karoo radio astronomy advantage area (DST 2009). The AGAC specifies the area for the Radio Frequency Interference (RFI) and identifies it as a free reserve. The reserved area requires low levels of RFI for the KAT7 radio telescope and for the development of the MeerKAT radio telescope. Additionally, low levels of RFI will be required for the Square Kilometre Array (SKA) development (DST 2009).

The development of CSP systems in SA must consider these regulations, which could affect the future development of CSP and potentially become constraints to successful uptake of CSP plants. Figure 2.3.1 shows the overall viable CSP sites, shalegas exploration sites and the RFI reserve sites. The proposed sites for this study do not interfere with RFI sites.

2.3.2 Hydraulic Fracturing

The shalegas exploration area is the area that is identified and estimated to have reserves of shalegas. Currently, the shalegas exploration is still in its initial stages. Figure 2.3.1 shows the shalegas identified area. This area overlaps with the CSP viable sites where CSP systems can be constructed. Also, proposed sites for this study fall within this area. Further, the viability and availability of shalegas in this area could increase the feasibility of baseload CSP plants in the future. These developments do not cripple the development of CSP systems and renewable energy systems in general. However, they need to be considered during power plant developments in order to comply with the laws.

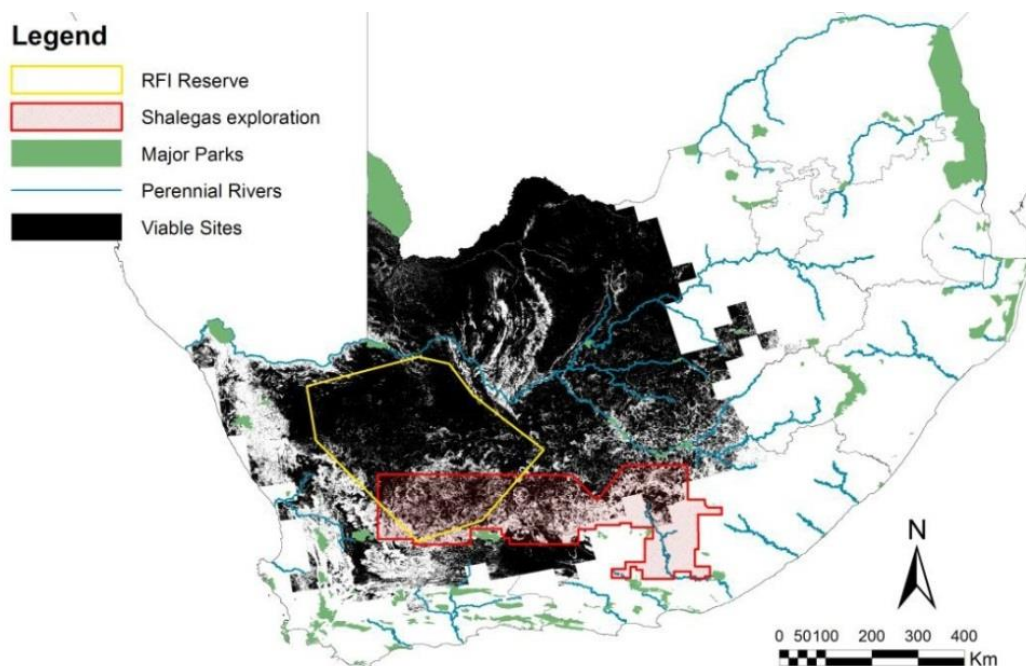


Figure 2.3.1: RFI reserve and shalegas exploration (Meyer 2012)

2.4 Previous Studies on CSP Dispatchability

What needs to be looked at carefully with regards to electricity generating technology capacity allocations is the issue of intermittency. Apart from the CSP system, all other renewable energy technologies allocated in the IRP are intermittent. That can potentially pose a drawback with regards to the load demand. The intermittent electricity generating technology typically requires backup capacity of the same amount in order to counter the intermittency. Additionally, the backup capacity is essential to counter for the low capacity factor of the technology. Another alternative is to investigate the feasibility of using storage with these systems.

The challenge with renewable energy uptake is in dealing with intermittency and the coincidence between the energy demand patterns and the solar resource availability (Gauché, et al. 2012).

A CSP system with TES is a dispatchable source of electricity. Large conventional energy systems, like coal plants, are usually restricted to 50 %–100 % operating range of full capacity (Denholm et al. 2013). Such a restriction may result in renewable energy to curtail in periods of high renewable energy resource. Furthermore, during the operation of conventional energy systems, ramping of the systems is avoided in order to minimise the operation and management costs (Denholm et al. 2013). CSP systems overcome this challenge by providing the ability to shift generation times to periods of high value.

Helman (2012) provides some insights about the value of CSP plants with TES by first giving a quantitative analysis of the value of a CSP plant with TES. The study concludes that 2–7 % of the value can be obtained through energy dispatch optimisation, as compared to discharge of storage after sunset (Helman 2012).

Figure 2.4.1 shows the typical electricity delivery from a CSP plant with three configurations: with no storage, with 2 hours storage not optimised for energy and with 2 hours storage optimised for energy. For the optimised configuration, the plant is able to hold the electricity production for later in the day when the electricity price is highest.

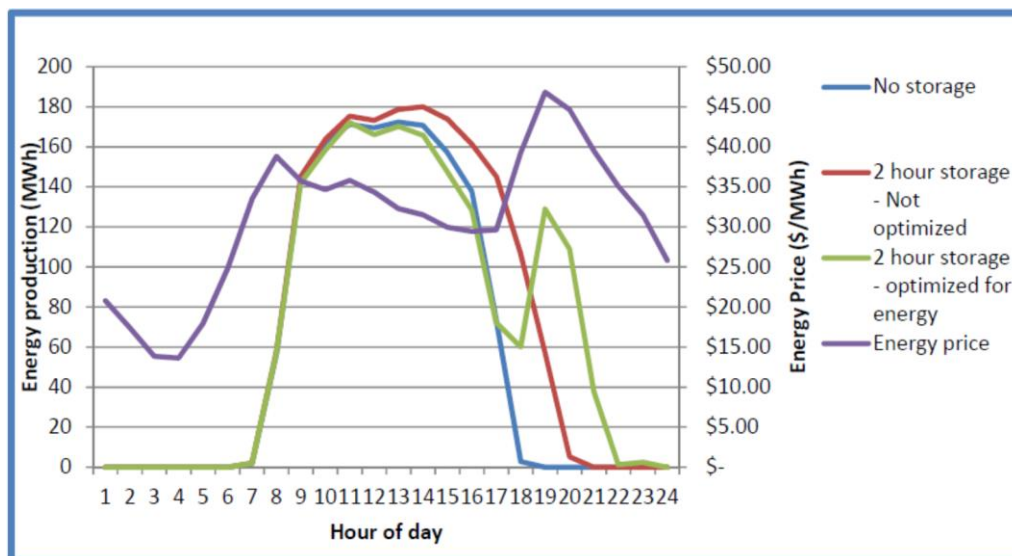


Figure 2.4.1: Energy production by hour of day (Helman 2012)

Sioshansi & Denholm (2010) presents an analysis of CSP with TES in different regions in the United States.

The study concluded that the operating profits vary with function of location and plant size. Sioshansi & Denholm (2010) conclude that the TES can increase the value of CSP by shifting the generation of energy to higher-priced periods and by allowing the utilisation of thermal energy from the solar field (Sioshansi & Denholm 2010). Sioshansi & Denholm (2010) states that good weather forecast allows for better energy dispatch processing which increases the value of CSP.

Figure 2.4.2 shows an example of CSP energy dispatch over one day. Also, it shows the electricity price profile with the highest value in the beginning and end of the day. The CSP plant is able to follow this profile using energy from the TES (Sioshansi & Denholm 2010).

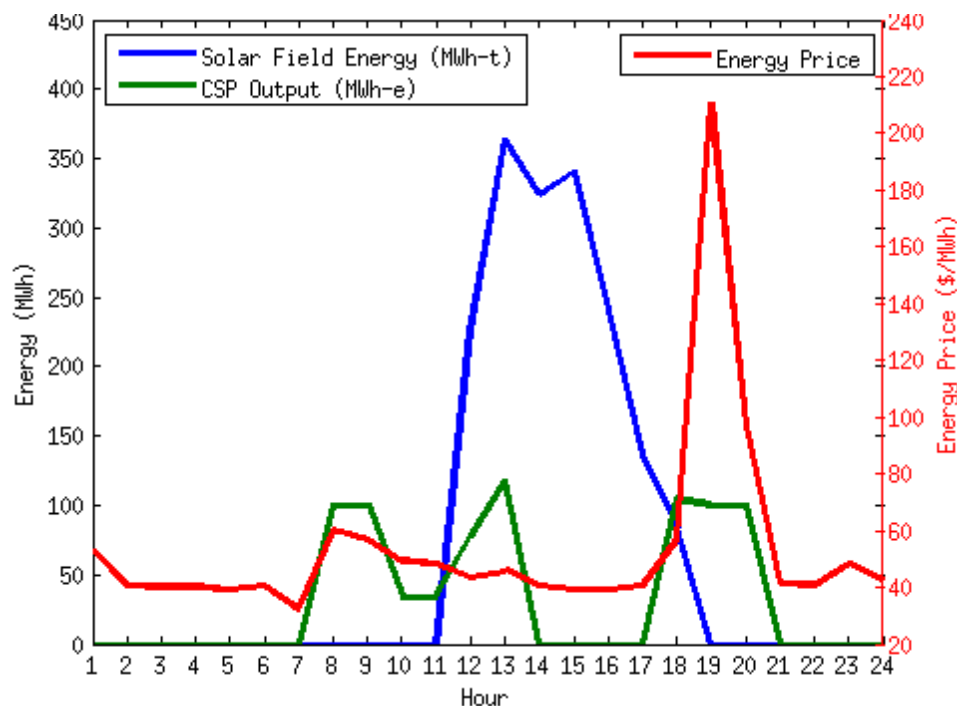


Figure 2.4.2: Sample of dispatch of a CSP plant with six hours of TES and a solar multiple of 2 (Sioshansi & Denholm 2010)

Gauché et al. (2011) present the modelling methodologies of the central receiver system. The study is based on the South African energy industry and seeks to provide a solution for a large scale roll-out of CSP. It evaluates the plant performance by considering the optical-to-thermal energy (Gauché et al. 2011). The study provides the point of departure for the analysis of a CSP plant's performance in South Africa.

Another study that is relevant to the work that is done here is the study by (Gauché, et al. 2012).

This study is about modelling dispatchability potential of CSP in South Africa. It concludes that a distributed CSP system has a potential of delivering dispatch power on demand.

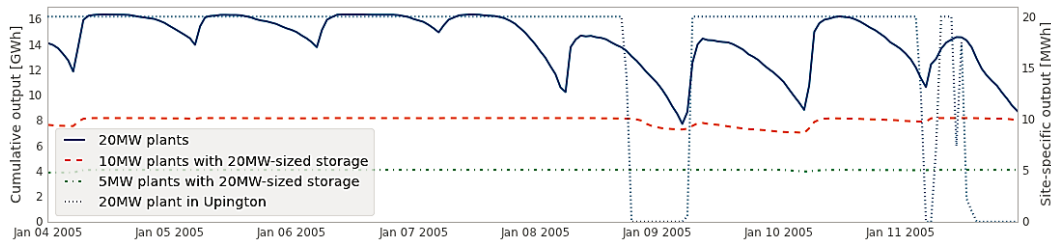


Figure 2.4.3: Summer results (only three models with baseline storage capacity in Upington) (Gauché, et al. 2012)

Figure 2.4.3 shows the model runs for a summer period. The figure shows the cumulative power production in the whole country from 823 CSP grid points (Gauché, et al. 2012). The Figure 2.4.3 also includes an individual power plant situated near Upington in the Northern Cape. Figure 2.4.3 shows that the fleet of 823 CSP distributed across the country manages to reach a production ceiling for several hours of the day but falls off over night as the storage gets depleted. The Upington CSP plant drops out significantly. The CSP plants with smaller power blocks show a potential for dispatchability (Gauché, et al. 2012).

Figure 2.4.4 shows the model runs for a winter period. The situation is different in winter as the electricity production from the fleet of plants fluctuates from maximum to minimum. The fleet of CSP plants with smaller power blocks show a potential for dispatchability for winter.

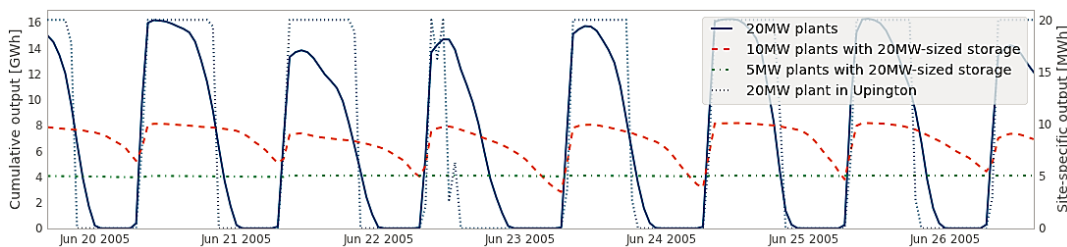


Figure 2.4.4: Winter results (only the three models with baseline storage capacity in Upington) (Gauché, et al. 2012)

2.5 CSP Systems Overview

This section gives an overview of the CSP technology. The CSP technology has a common operational mechanism that requires concentration of radiant flux. The general principle of concentration of the radiant flux by the concentrating systems requires a bigger solar reflector that reflects the flux to the smaller receiver.

In general, the operation of the solar collector deals with the energy balance of the solar energy that is absorbed and lost by the collector (Stine & Geyer 2001). Moreover, the heat losses on the receiver are directly proportional to the area of the receiver; so concentrating the flux to a smaller receiver allows the system to operate at high temperatures and still achieve less thermal energy losses.

2.5.1 Stirling Dish System

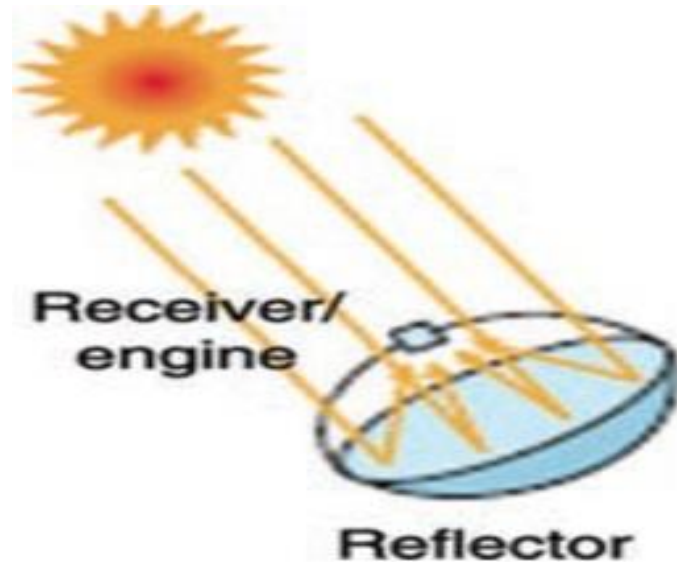


Figure 2.5.1 Stirling dish system configuration (Heap 2011)

The parabolic dish system is a point focusing system. It has reflectors that are placed on the curved dish surface and reflect the sun's rays to the receiver focal point where the engine is placed, as shown Figure 2.5.1. This system is a two-axis tracking system that faces the sun and tracks it during the course of the day. This system can be utilized for different applications; however, the most common application for a dish system is with the Stirling engine, where the energy collected by the dish is used to power the Stirling engine, which is situated at the focal point. Hence, the dish system is also known as the Stirling dish system. The Stirling engines have a relatively high efficiency with demonstrated solar to electric efficiency of 29.4 % (SolarPACES 2012a). Additionally, the Stirling dish is characterised by autonomous operation and modularity (SolarPACES 2012a), which allow these systems to be installed as stand-alone, off-grid Stirling dish systems or grouped together.

Currently, the system capacity for the Stirling dish system ranges from 9 kW to 25 kW (SolarPACES 2012a).

A 25 kW system operating under the DNI of $1\,000\text{ W/m}^2$ has a system concentrator with a diameter of 10 m (SolarPACES 2012a). The drawback with the Stirling dish is that it does not allow for energy storage. This makes it irrelevant for consideration in this study.

2.5.2 Linear Fresnel System

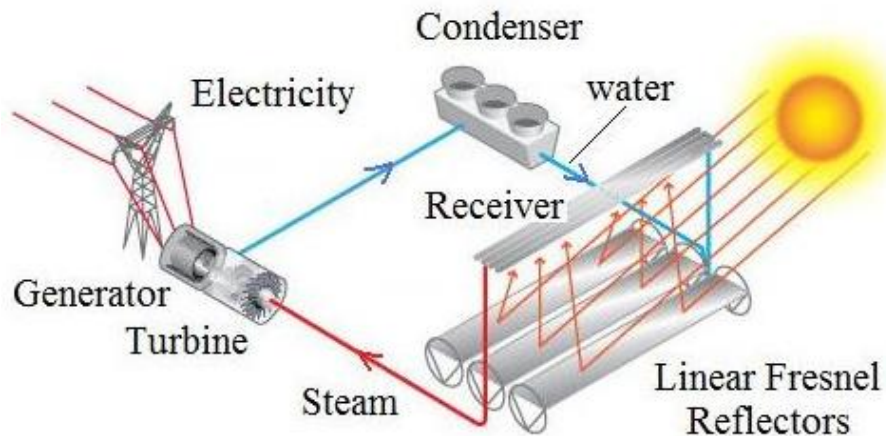


Figure 2.5.2: Linear Fresnel system configuration (US DoE 2013)

The linear Fresnel system consists of a solar field made up of Fresnel reflectors. The mirror reflectors are single-axis tracking that reflect the sun's rays to the linear stationary receiver, as shown in Figure 2.5.2. The reflector mirrors may have a small curvature, which is achieved by mechanical bending (Häberle et al. n.d.). The receiver of the Fresnel system is fixed and only the reflectors rotate. This eliminates moving parts and couplings and allows for direct steam generation. However, there is on-going research about utilising molten salt as a heat transfer fluid (HTF) (Häberle et al. n.d.).

The linear Fresnel system offers an advantage with regards to land usage. The reflectors are placed next to each other, resulting in efficient land use, and the compact nature of the system results in reduced wind loads. The linear Fresnel systems that are currently operational are still only research facilities. However, these facilities are proving the potential of the system. An example of an operational Fresnel system is the 150 kW system operated by BBEnergy (Gonzalez & Nell 2013). BBEnergy is a registered Energy Service Company to Eskom, and it is contracted to construct and operate the linear Fresnel system on behalf of Eskom (Gonzalez & Nell 2013). This system is in the final stages of testing, and the feedback is that it is performing well. An important note about this system is that it is designed in South Africa and has 95 % local component content (Gonzalez & Nell 2013).

Currently, the demonstrated Fresnel CSP technology has direct steam configuration. The utilisation of molten salt as a HTF in Fresnel technology has not yet been demonstrated as it is still in research phase. This study aims to demonstrate dispatchability potential of CSP technology. The utilisation of the Fresnel technology, which requires an additional molten salt loop in order to store energy, is not considered for this study.

2.5.3 Parabolic Trough System

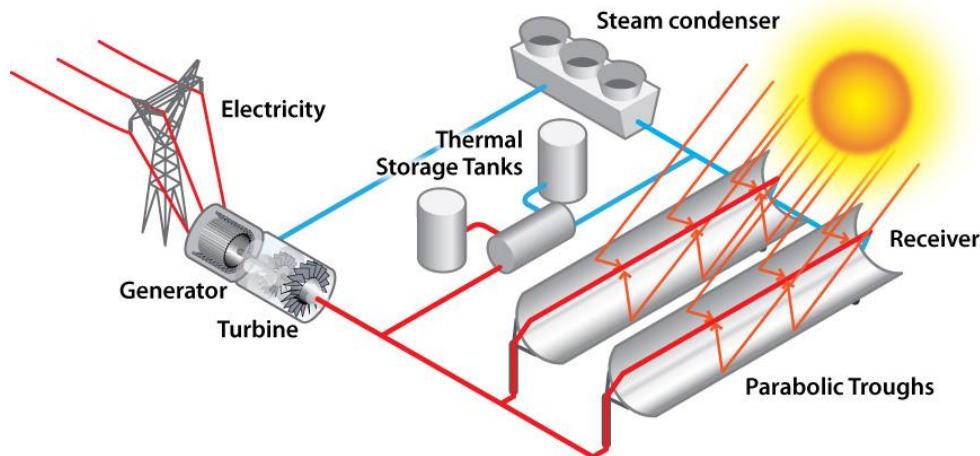


Figure 2.5.3: Parabolic trough system configuration (US DoE 2013)

The parabolic trough system consists of north-south tracking, horizontal-axis, parabolic curved mirrors that have a linear absorber running through them. These mirrors reflect the sun's rays to a linear absorber tube located at the focus of the parabola (see Figure 2.5.3). The commercially operating parabolic trough system utilizes the Rankine cycle. The hot HTF from the field serves as the higher temperature source in the heat exchanger to generate steam.

The commercial parabolic trough uses synthetic oil, which limits the maximum operating temperature to approximately 390 °C (Gary et al. 2011). Even though the trough system is commercially matured, the operating temperatures still provide an opportunity to improve the trough system. Such improvements could be in the form of operational or financial improvements. Currently, there is research underway to utilize steam as both the HTF and working fluid-direct steam generation (DSG) (SolarPACES 2012b). This improvement will automatically benefit the system by eliminating the separate HTF and the heat exchanger that generates steam. The initial results show that the DSG will likely be more complicated due to the higher operating pressures and the lower fluid flow rates (SolarPACES 2012b). Another potential improvement regarding operating temperatures is the utilization of molten salt as the HTF, which will enable high operating temperatures of the molten salt, estimated at 500 °C, and the possibility of a direct storage system.

The challenge is the freezing temperatures of the molten salt (Gary et al. 2011). Currently, the demonstrated capital costs are 4 500 \$/kW for a 100 MW plant without storage (Gary et al. 2011). Gary et al. (2011) predict that a 250 MW plant with 6 hours of storage will have capital costs of 7 870 \$/kW in 2015 and 6 530 \$/kW in 2020, and the LCOE will be 19.0 c/kWh and 11.4 c/kWh respectively (Gary et al. 2011).

2.5.4 Central Receiver (Tower) System

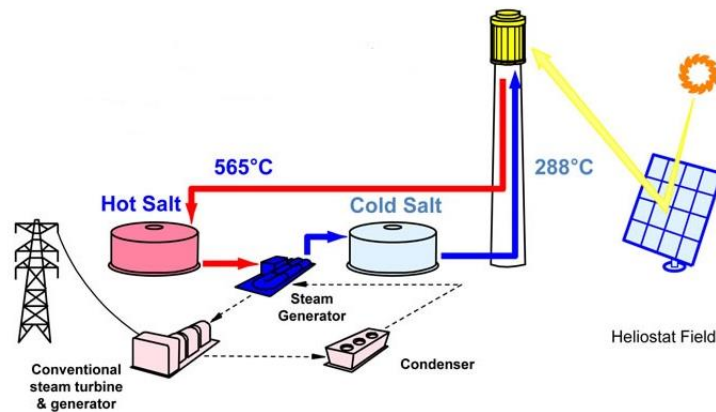


Figure 2.5.4: Central receiver system configuration (Heap 2011)

The central receiver (tower) system is a point focusing, two-axis tracking system. It consists of many individual mirror reflectors—also known as heliostats—that track the sun's rays during the course of the day and reflect them to the receiver situated at the top of the tower (see Figure 2.5.4). The receiver absorbs the solar energy and transfers it to the heat transfer fluid. The ratio of the size of the solar field and the size of the receiver results in a high concentration ratio for the central receiver system, which allows the tower system to achieve high energy density in the receiver and thus operate at high temperatures.

The DSG and the molten salt are used as HTF in the operation of the tower with recorded operating temperatures of 550 °C and 565 °C respectively (Gary et al. 2011). These temperatures are possible because of higher concentration ratios and the smaller amount of piping in the tower. Research shows that operating temperatures of 1 000 °C are possible, depending on the HTF medium (Gary et al. 2011). The most utilized commercially available tower system uses molten salt as the heat transfer fluid, with the salt in the cold tank at 290°C and the temperature of the hot tank at 565 °C (SolarPACES 2012c). Using molten salts as both the HTF and storage medium allows for direct storage, which improves the efficiency of the system. The two tank molten salt system is highly efficient, with recorded round trip efficiency of 98 % taken at the Solar Two plant (Gary et al. 2011). The TES plays a huge role in the operation of the tower system because it creates a dispatchable source of energy.

Gary et al. (2011) predict that the capital costs of the tower system will decrease significantly as the technology improves and capacity increases. Capital costs are predicted to be 5 940 \$/kW in 2015 for 100 MW with 6 hours TES and 6 430 \$/kW in 2020 for a 150 MW with 14 hours TES. The predicted LCOE are 14.4 c/kWh and 9.8 c/kWh respectively (Gary et al. 2011).

2.5.5 Comparison: CSP Tower vs CSP Trough

The central receiver has the advantage of having a direct storage system, which results in lower capital costs of the TES, and it is commercially available with the TES. The utilization of thermal storage increases the capacity factor of the CSP system. Over and above that, thermal storage allows the CSP plant to deliver dispatchable energy based on demand. Currently, the state-of-the-art direct system is the system that was commissioned in 2011 on the Gemasolar power plant (NREL 2011). In the indirect system, the HTF is decoupled from the storage medium, thereby requiring a heat exchanger between the HTF and storage medium. Table 2.4 shows the two types of storage system configurations: direct storage and indirect storage. As the Table indicates, the advantage of utilizing the direct storage system is that the salt mass is reduced by a third compared to the indirect storage system.

Table 2.4: Commercially available two tank TES

| Item | Gemasolar (Tower) | Andasol 1 (Trough) |
|------------------|-------------------|--------------------|
| Type of system | Direct storage | Indirect storage |
| Thermal capacity | 1 000 MWh | 1 010 MWh |
| Salt mass | 8 500 tones | 28 500 tones |
| Cold tank temp | 290 °C | 292 °C |
| Hot temperature | 565 °C | 386 °C |

2.6 Conclusion

The literature survey shows the current state and future state of electricity industry in South Africa. By reviewing the IRP, the literature survey shows that the capacity allocation to CSP is minimal. Perhaps there are more capacity allocations to other electricity generating technologies like OCGT, which is seen in the IRP as the potential peaking solution. However, future fuel costs are likely to increase. The literature survey presents the work that has been done on other studies to illustrate the dispatch potential of CSP technology, considering the state of the art CSP technology – direct salt central receiver.

3 Supply and Demand for Peaking

This chapter provides the method used to obtain the results in this study and gives an overview and technical description of the energy systems that were modelled: the OCGT system and the CSP system. The LCOE of the CSP system are compared with that of the OCGT system, and a discussion about the LCOE of these systems follows.

3.1 Load Demand for Peaking

To model the performance of the CSP system, the peak electricity demand was first determined. The peak load demand of this model was assumed from Eskom’s 2010 national load demand. This load demand indicates the annual national load requirement from Eskom, and it is provided as hourly load demand data (Gauché 2012).

The peak load demand was assumed to be a fraction of the maximum hourly load demand of each day. The daily maximum hourly demand was multiplied by this baseload fraction. The baseload fraction indicates how much of that hourly load demand will be from non-peaking sources. For this study, a baseload fraction of 90 % of the maximum hourly demand was set as the baseload demand of the day. This is not a true baseload, but it is used in this study to test the method. Further, the technique does more than supply peak electricity demand; it also supplies some mid-merit electricity demand. Figure 3.1.1 shows a schematic illustration of how the peak load is assumed for this study.

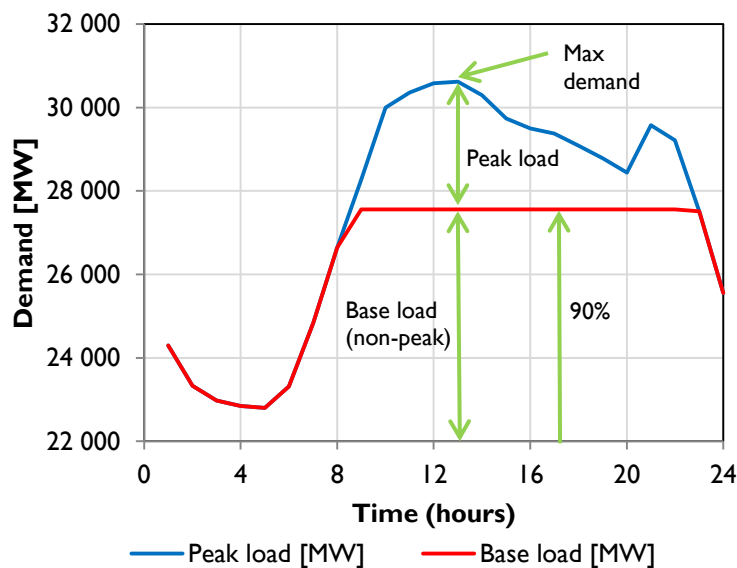


Figure 3.1.1: Peak load definition schematic illustration

Supply and Demand for Peaking

The reason for using the above mentioned method is to allow the CSP plant to consistently deliver the required amount of energy throughout the year without being influenced by the seasonal weather. The method allows the CSP plant to be utilized sufficiently throughout the year. It assumes that some additional baseload capacity is available in parts of the year with higher electricity demand. The two following graphs (Figures 3.1.2a and 3.1.2b) show the load demand for a week in January and a week in June. The graphs indicate that the load demand is lower in January than in June, but the solar resource in January is higher compared to June. The baseload multiple allows the CSP to be utilised during all seasons.

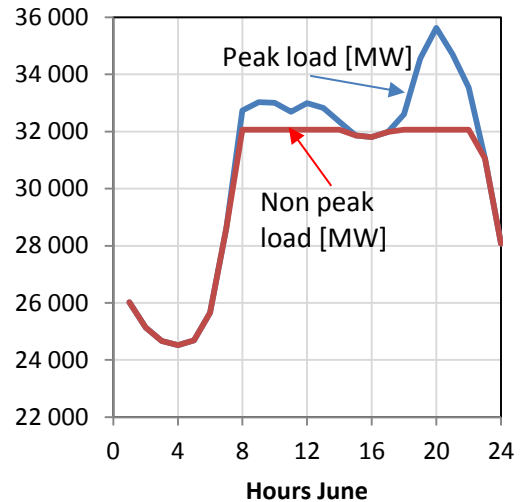
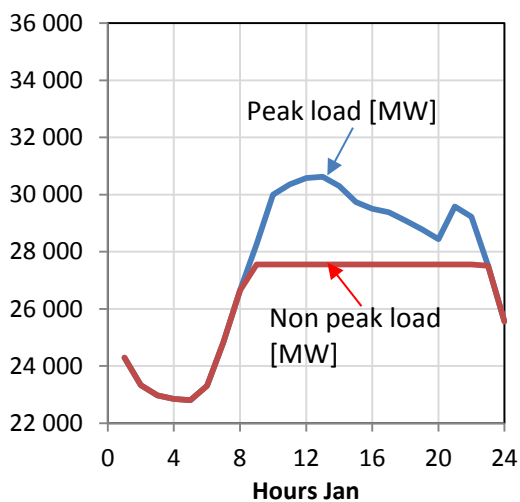


Figure 3.1.2a: January load demand **Figure 3.1.2b: June load demand**

Figure 3.1.2a shows the baseload demand and the peak load demand for a week in January. Although the baseload demand is lower in January, the baseload multiple allows the CSP plant to be effective because the peak load is distributed over a longer period. This peak load distribution results in a higher energy supply from the CSP system, which is able to contribute effectively to this demand because the solar resource is higher in January.

Figure 3.1.2b shows the baseload and the peak load demand for a week in June. Although the load demand in June is higher, it is not distributed over a longer period. This results in less energy demand as compared with January. A CSP system is able to contribute effectively because there is less solar energy and less peak energy demand.

3.2 CSP Central Receiver Plant

The Gemasolar CSP plant is a central receiver system with a turbine rating of 20 MW and full load storage of 15 hours. It is situated in the South of Spain in the region of Andalusia, Sevilla. This CSP plant was commissioned in 2011, and during its first summer it operated at full load production for 24 continuous hours. This was a significant achievement in the CSP industry as it highlighted the capabilities of CSP technology with significant TES. The region where the Gemasolar plant is located is known to have one of the best solar resources in Spain of 2 172 kWh/m²/year (NREL 2011). The Gemasolar CSP plant was used as the reference CSP power plant in this study, and primary component sizes were adapted in this study.

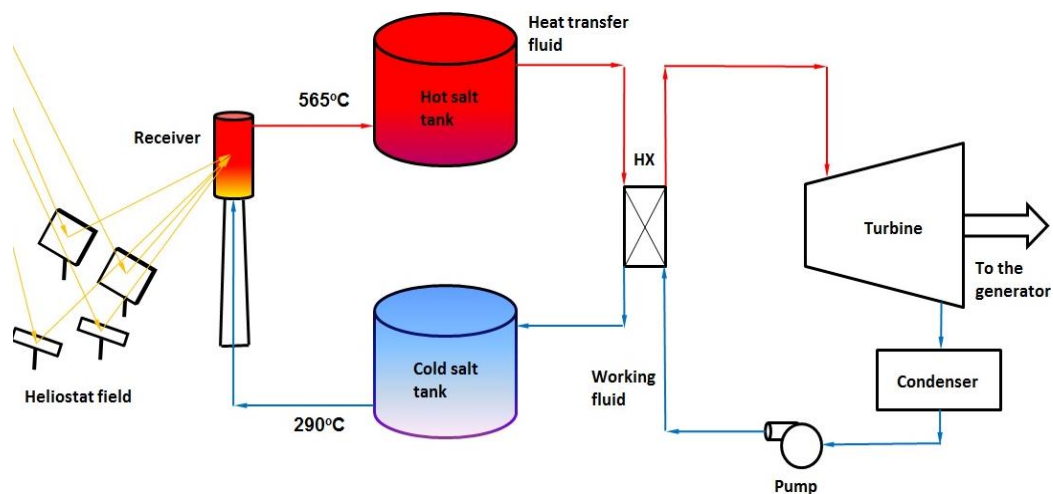


Figure 3.2.1: CSP plant configuration

Figure 3.2.1 illustrates the key components of a central receiver system based on the Gemasolar plant. This CSP system has a primary loop, with a salt HTF and a two tank system. The second loop, the traditional superheated Rankine cycle configuration, makes energy collection and electricity generation largely independent.

3.2.1 Gemasolar Power Plant

Figure 3.2.2 shows the aerial view of the Gemasolar CSP plant. Table 3.1 provides a summary of the Gemasolar plant specifications. This information was obtained from the NREL/SolarPACES database (NREL 2011), the reference plant for this study.

As indicated in Table 3.1, the Gemasolar plant is a 20 MW, 304 750 m² heliostat aperture and 15 hour TES plant. In order to meet the assumed load in this study, these parameters were scaled up or down in the model. The scaling up of the plant parameters are discussed later in section 4.1.10, Power Plant Scaling



Figure 3.2.2: Gemasolar CSP power plant (Torresol Energy 2013)

Table 3.1: Gemasolar power plant specifications

| Item | Value |
|-----------------------------|-------------------------------|
| Land area | 195 ha |
| Electricity generation | 110 GWh/year (forecast) |
| Thermal cycle efficiency | 40 % |
| Cost | 230,000,000 Euro |
| Heliostat aperture area | 304, 750 m ² |
| Number of heliostats | 2 650 |
| Heliostat size | 120 m ² |
| Tower height | 140 m |
| Receiver inlet temperature | 290 °C |
| Receiver outlet temperature | 565 °C |
| Turbine capacity | 20 MW |
| Cooling system | Wet cooled |
| Storage | 2 tank molten salt (15 hours) |

3.2.2 Thermodynamic Cycle

The Gemasolar plant uses the Rankine cycle, which is the thermodynamic cycle that was assumed for the present study. The Rankine cycle is widely utilized in the electricity industry in electricity systems such as coal, nuclear and CSP plants. The working principles involve using water/steam as the working fluid. Energy is transferred to the water from a higher temperature source to generate steam, which is then sent through the turbine to generate electricity.

The CSP technical model that is used in this study is based on the Chambadal-Novikov efficiency. The Chambadal-Novikov efficiency, which is discussed in 4.1.8, shows good prediction of the Rankine cycle performance. Figure 3.2.3 shows the T-s diagram of saturated steam (3-4-1-2-3) and the T-s diagram of superheated steam (3-4-1'-2'-3). Rankine cycle based power plants ramp slowly, thus not good for dispatch. Additionally, they are not good for part load. This is mostly boiler related, and CSP technology does not have this problem (Black&Veatch 2012).

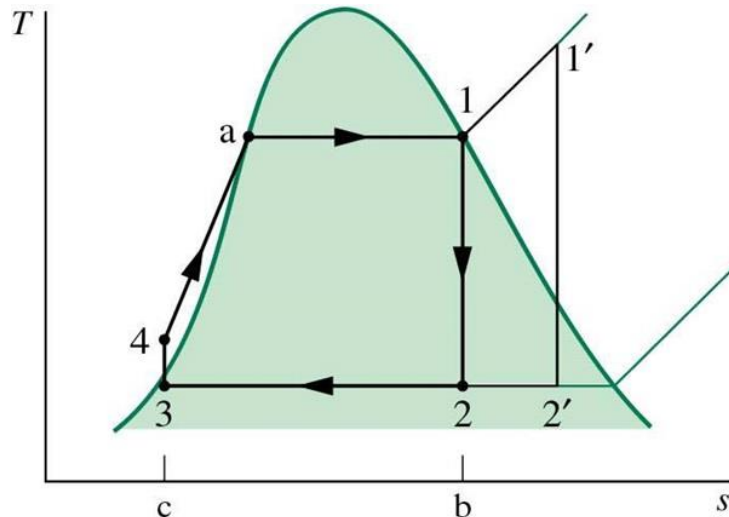


Figure 3.2.3: T-s diagram of saturated and superheated steam Rankine cycle (MAE 2013)

3.3 Open Cycle Gas Turbine (OCGT)

OCGT systems are commercially available, mature and utilized in the power industry (Brinckerhoff 2008). These systems have proven versatility in industries such as aviation, oil and gas and power generation. The IRP identifies the OCGT as the future peaking station which could be run on natural gas in the long-term. However, the IRP predicts that the OCGT will be run on diesel in the short-term due to unproven adequate reserves of natural gas and lack of infrastructure (DoE 2011). Currently, diesel powered OCGT systems are used as peaking stations in South Africa (DoE 2011).

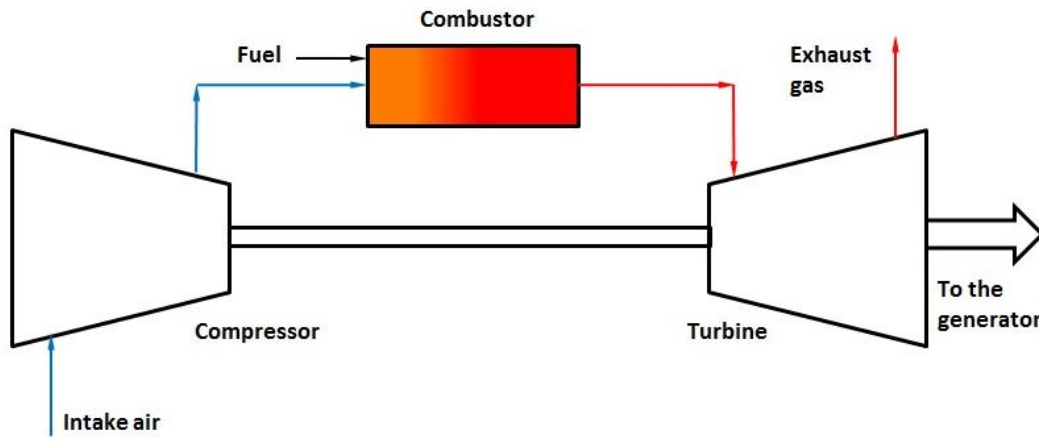


Figure 3.3.1: Open Cycle Gas Turbine (OCGT) configuration

Figure 3.3.1 shows a typical OCGT system. The key components of the OCGT are the compressor module, the combustor, the turbine and the generator. The two most important inputs of the OCGT are the compressed air and the fuel. The OCGT operation particularly comprises the compression of air in the compressor module by the compressor. This compressed air is then mixed with fuel in the mixing chamber/combustor and ignited. The ignited gas mixture gains significant potential energy by increasing the temperature and the pressure. The ignited gas mixture is then put through the turbine, thereby turning the turbine. The turbine shaft rotates and drives the compressor, and the power that is available on the turbine shaft is then used to drive the electricity generator.

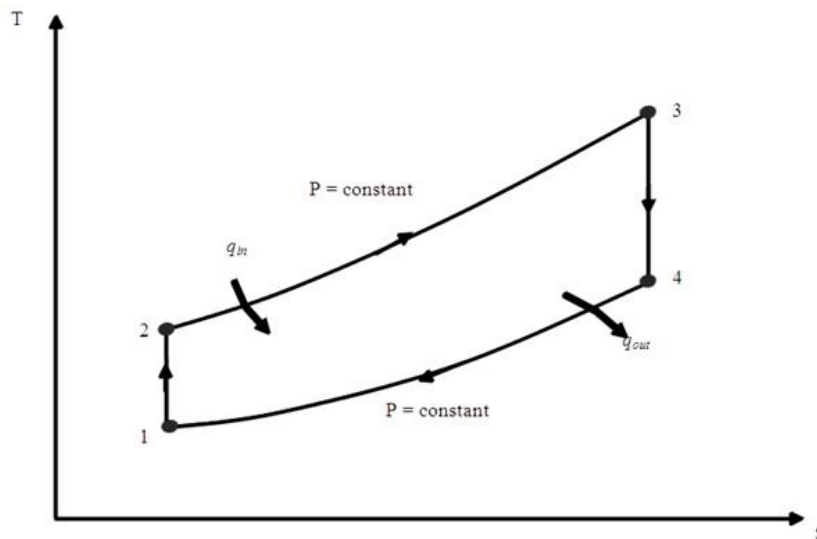


Figure 3.3.2: T-s diagram of Brayton cycle (Ogbonnaya 2004)

Figure 3.3.2 shows the T-s diagram of the Brayton cycle (1-2-3-4-1). The technical model of the OCGT is based on the Brayton cycle and resembles this T-s diagram. The OCGT technology has a quick start ramp rate of 22.20 %/min to full load capacity (Black&Veatch 2012).

3.4 Levelised Costs of Electricity

The Levelised Costs of Electricity (LCOE) allows the energy generation systems to be compared on weighted average costs. The LCOE calculation is done by net present value method, which calculates the investment expenses and operation during the life time of the plant. The present values of all the expenses are divided by the present values of all the electricity produced. The costs are for the total investments and the operational expenses over the lifetime of the power plant. LCOE aims to provide a fair comparison of electricity generation technologies.

The LCOE analysis is used in this study to determine the feasibility of utilising CSP plants as peaking power plants in South Africa. This is done by obtaining the LCOE of the CSP system and comparing it with the LCOE of the OCGT system. Utilizing the LCOE to compare different energy generation technologies is adequate because it allows for a technology comparison based on the weighted average costs basis.

The equation (3.1) is the LCOE formula used in this study. The equation (3.1) was adapted from the Crespo et al. (2012) report.

$$LCOE = \frac{\sum_{t=1}^n \frac{I_t + M_t + F_t}{(1+r)^t}}{\sum_{t=1}^n \frac{E_t}{(1+r)^t}} \quad (3.1)$$

| Item | Description |
|-------|--|
| I_t | <i>Investment expenditure in the year t</i> |
| M_t | <i>operations and maintenance expenditures in the year t</i> |
| F_t | <i>fuel expenditures in the year t</i> |
| E_t | <i>electricity generation in the year t</i> |
| r | <i>dicount rate</i> |
| n | <i>life of the system</i> |

The LCOE considers the total expenditure costs divided by the electricity generated. The total costs include the investment costs, fixed and variable maintenance costs, and operational costs over the lifetime of the plant. The present values of total expenses are divided by the present values of total electricity generation costs.

3.4.1 Levelised Costs of Electricity – OCGT

The initial analysis of the OCGT technology suggests that OCGTs generate electricity at a cost in excess of 5.00 ZAR/kWh. The OCGT technology is currently run using diesel and the diesel prices are expected to increase in the future.

3.4.2 Levelised Costs of Electricity – CSP

The initial analysis on the CSP technology suggests that the CSP generates electricity at a cost in excess of 1.80 ZAR/kWh. This is lower than the current costs of OCGT technology that is used to service evening peaks. Additionally, the CSP costs are below the prices of the first windows of the Renewable Energy Independent Power Producer Procurement Programme.

3.5 Conclusion

The supply and demand for peaking illustrated the method of assuming peak load for the study. This chapter revealed that the electricity demand load profile for South Africa is predictable. Currently, the OCGT technology is used to supply the peak load. However, the CSP technology may have a potential to be used as peaking technology due to the predictability of electricity load profile. LCOE, which is described in this chapter, is identified as a suitable analysis tool for determining the feasibility of using CSP technology as a peaking system.

4 Technical Model Development

This chapter gives an overview of the technical models that were used to obtain results for this study. These models are the CSP and OCGT. The models that were used along with their operating parameters are discussed in this chapter.

4.1 CSP Plant Model Development

The CSP model used and adapted for this study is a systematic model of the CSP tower system by Gauché, al. (2012). The average hourly solar resource data is used as inputs to evaluate the plant performance. This type of modelling evaluates the plant performance by considering the optical-to-thermal energy conversion. The key inputs for the modelling purposes are the DNI solar resource, the solar field configuration, ambient temperature, wind speed and the receiver operating temperature.

The model from Gauché, et al. (2012) is adapted and used for this study. The model has been validated using the results from the eSolar Sierra tower plant in California, and it matches the expected annual performance of the Gemasolar plant reasonably well (Gauché, et al. 2012). The model aims to generally replicate the Gemasolar plant with the understanding that it is a real plant proving the ability to dispatch (NREL 2011). The model allows the turbine rating and storage reference hours to be modified.

This section discusses the optical and thermal performance of the model by considering the optical losses of the solar field and the thermal losses of the CSP system. Key components of the CSP plant are discussed in this section with emphasis put on the performance of the following components:

- Heliostat field optics
- Receiver energy balance
- Storage system energy balance
- Power block

4.1.1 Heliostat Field Background

The solar field consists of multiple tracking reflectors called heliostats, which reflect the solar radiation to the tower's receiver. For an effective operation of the heliostat, it should reflect the maximum possible solar energy to the receiver. This operation is impacted by various effects such as surface quality, field layout, etc.

4.1.2 Heliostat Optical Losses

The reflective area for a state-of-the-art commercial heliostat consists of a low iron glass with back reflective material. The low iron allows maximum energy transmission through the glass. The glass improves the performance of the heliostat over its life time by reducing surface damages on the reflective material, which reduce reflectivity. The reflective material reflects the maximum solar radiation. Silver, gold and aluminium are some of the best reflective materials with high specular reflection. Silver is the preferred reflective material, however, because its optimal performs over the solar spectrum (Stine & Geyer 2001).

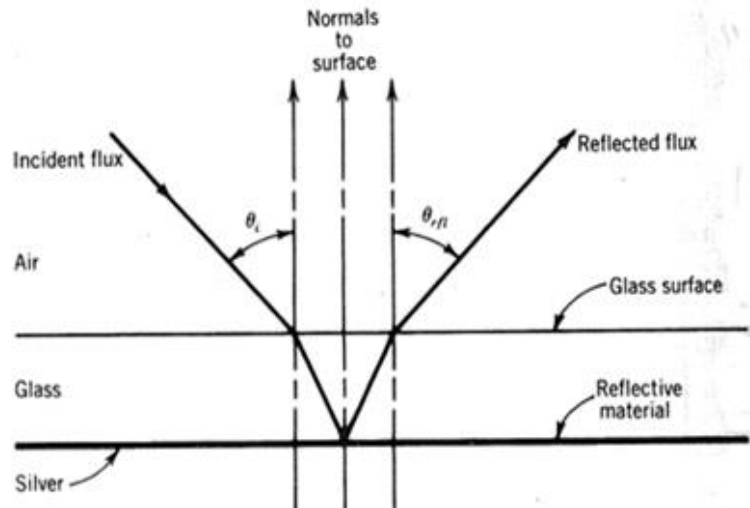


Figure 4.1.1: Heliostat optics (Stine & Geyer 2001)

Figure 4.1.1 shows the Snells law. The Figure 4.1.1 illustrates the optics of the heliostat with the glass and back reflective surface. The low iron mirror absorbs less energy and allows the maximum solar rays to be refracted, while the reflective material allows the maximum solar radiation to be reflected. The efficiency of these aspects determines the optical efficiency of the heliostat.

4.1.3 Heliostat Field Losses

The performance of a heliostat field can be adversely affected by various losses. These losses were factored in the development of the model. These losses include the following:

- Cosine effect
- Blocking and shading
- Spillage losses
- Atmospheric attenuation
- Heliostat availability
- Field tracking accuracy

Cosine Effect

Cosine losses are due to the angle between incident radiation and the surface normal to the heliostat. Figure 4.1.2 illustrates the effect of cosine loss on a heliostat. To determine the cosine losses from the heliostat, the angle between incident radiation and the heliostat normal is required. As this angle decreases, the size of the reflected image increases and vice versa. Equation (4.1) shows the reflected radiation ($\dot{Q}_{heliostat}$) from the heliostat is a product of cosine of (α), the incident radiation (I_{beam}) and the heliostat surface area ($A_{heliostat}$).

$$\dot{Q}_{heliostat} = \cos(\alpha) * I_{beam} * A_{heliostat} \quad (4.1)$$

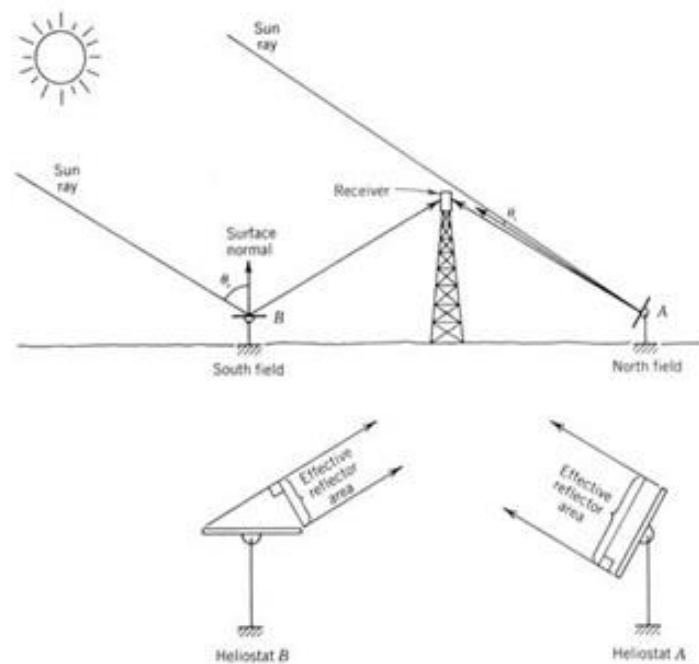


Figure 4.1.2: Cosine effect on the heliostat spectrum (Stine & Geyer 2001)

Blocking and Shading

Blocking and shading is caused by the position of heliostats in relation to other heliostats. Shading is caused by a heliostat casting a shadow on another heliostat located behind it relative to sun. This is prevalent at low solar altitude angles during sunrise or sunset when not all the solar beam radiation reaches the heliostat.

Blocking occurs when a heliostat closer to the tower partially blocks the reflected beam from another heliostat behind. Figure 4.1.3 illustrates the processes of blocking and shading from the heliostat.

Because these processes interfere with the amount of solar energy that reaches the receiver, the efficiency of the solar field is reduced. These losses are a function of the sun angle, tower height and heliostat spacing. Optimization of the solar field reduces these losses, thereby improving efficiency.

Other Losses

The atmospheric attenuation losses are also referred to as the scattering of the solar beam radiation. This is an atmospheric loss not accounted for in the ground measured irradiation and occurs between point of reflection and receiver. These losses are dependent on the distance of the heliostat from the receiver, humidity and plant elevation. Spillage losses represent the amount of reflected sun rays that do not reach the receiver. These losses are heavily influenced by the tracking accuracy of the heliostat.

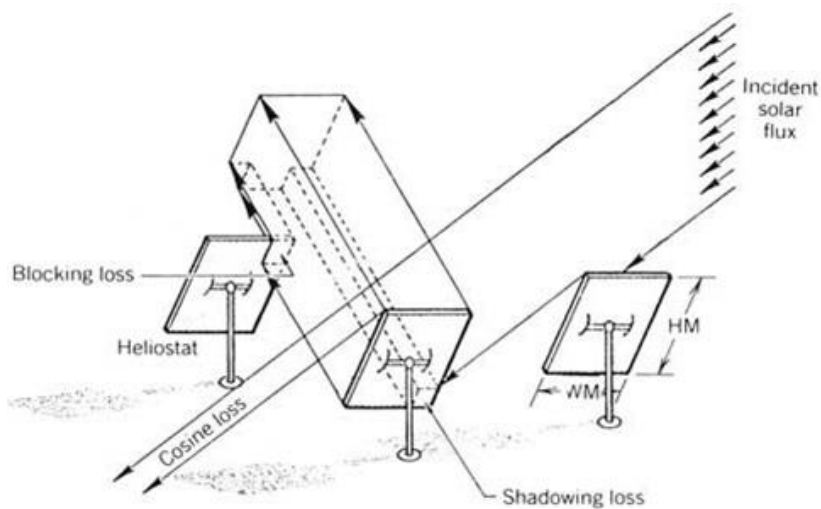


Figure 4.1.3: Blocking and shading from the solar field (Stine & Geyer 2001)

Solar Field Operating Parameters

In an effort to keep the model simple, the method developed by Gauché et al. (2011) was used to determine the optical losses. This method accounts for the above mentioned optical losses from the solar field and the heliostat. The first requirement of the plant model is the continuous determination of sun position. The solar time, which is based on the angular motion of the sun across the sky, is derived; it contains standard time, longitudinal corrections and the equation of time. The equation of time is derived by Spencer (Gauché et al. 2011). From the solar time, the hour angle, which is the conversion of solar time into angle, is derived. After that the zenith angle and the azimuth angles are derived. These angles provide the incidence ray to the heliostat module, and the receiver atop of the tower provides the reflected incidence target.

The implementation of the position of the sun as well as the remaining model description has been documented by (Gauché et al. 2011) and is provided here in summary.

The circular-like heliostat field of the Gemasolar plant reveals that the optical performance is dominated by the zenith angle and has a very low dependence of the solar azimuth angle. This makes it convenient to express the optical efficiency as a single polynomial for quicker and simpler analysis, an important consideration when running CSP models for scenario analysis. Equation (4.2) is thus only a function of zenith angle and is used for all plant models, assuming that the heliostat field and tower remain unchanged (Gauché et al. 2011). An illustration of the Zenith angle calculation is shown in Appendix A.

$$\eta_{opt} = 0.4254\theta_z^6 - 1.148\theta_z^5 + 0.3507\theta_z^4 + 0.755\theta_z^3 - 0.5918\theta_z^2 + 0.0616\theta_z + 0.832\theta \quad (4.2)$$

The heliostat layout of the Gemasolar is not available for this study, but it is approximated using plant parameters in Table 3.1. The zenith angle domination analysis of the circular solar field like Gemasolar is used to produce the curve fit that is shown in Figure 4.1.4.

Solar field optical losses

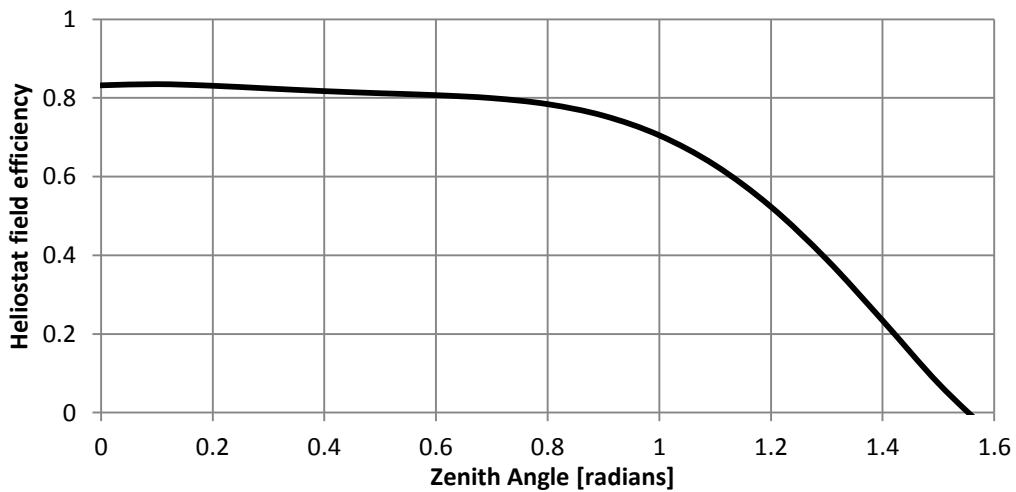


Figure 4.1.4: Representation of optical (cosine, blocking, shading, etc.) losses curve fit (Gauché, et al. 2012)

4.1.4 Receiver Background

The solar radiation that is reflected by the heliostats to the receiver is converted to thermal energy and transferred to the heat transfer fluid.

The Gemasolar power plant utilises an external receiver that is atop a 140 m tower. The thermal capacity of the Gemasolar receiver is 120 MWth (NREL 2011).

The external tube receivers are the most mature and utilised receivers in the CSP industry. The current receivers, which can also be referred to as the second generation external receivers, utilise the molten salt as the heat transfer fluid. These second generation external receivers have advantages resulting from the utilization of molten salt that allow for direct thermal storage. The lifecycle is not proven yet, but accelerated tests and promising experience indicates the predicted performance (Lata 2008). For an effective system, the tubes should have high thermal conductivity. Compared to steam, the molten salt can accommodate higher solar flux for the same receiver size.

4.1.5 Receiver Geometry

The receiver that was modelled for this study is a commercially available external receiver that consists of vertical tubes filled with the heat transfer fluid. The size of these tubes can vary from 0.02 m to 0.045 m. These tubes are joined together to form small rectangular panels. The number of tubes in each panel determines the size of each panel, and this is chosen carefully by optimizing the absorption of energy and the size of the receiver diameter. The tubes are coated with a high absorptivity material, which can reach 94 % and 95 % at all radiation wavelengths (Pacheco, J.E et al, 2002).

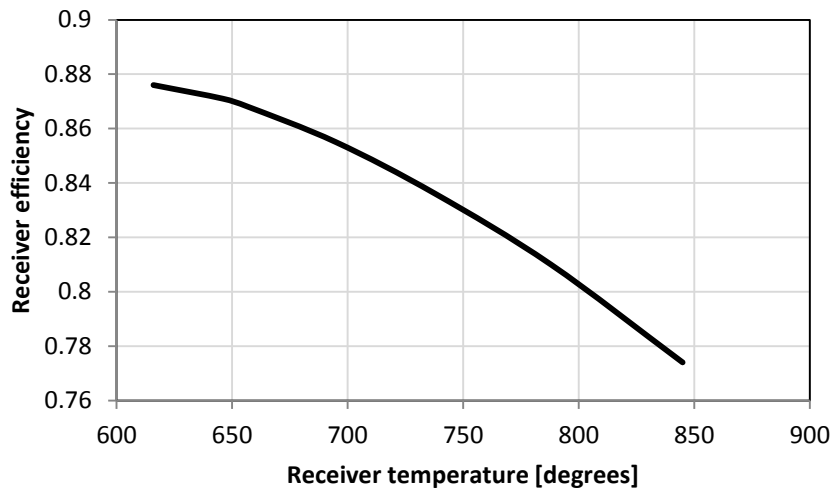


Figure 4.1.5: External receiver efficiency curve (Lata 2008)

Figure 4.1.5 illustrates the efficiency of the external receiver. For the state of the art external receiver, the operating temperature of the receiver is 565 °C. Figure 4.1.5 shows that the receiver is able to operate at higher temperatures.

However, it operates at this temperature because it is limited by molten salt and the power block operating temperature. Care is needed in the operation of the receiver for thermal stresses due to many factors of controlling flux distribution, flow rate. etc. (Lata 2008).

4.1.6 Receiver Energy Balance

The energy balance on the receiver is performed to determine the energy that is transferred to the HTF and sent to the TES. The equations (4.3 and 4.4) are used to perform the energy balance of the receiver. The model utilizes a fixed output temperature of 565 °C for the receiver based on the operating temperature of the Gemasolar plant. The inlet and outlet temperature of the receiver are fixed and the radiation component is solved for this range (Gauché, et al. 2012). The HTF enters the receiver at 290 °C and leaves the receiver at 565 °C.

$$\dot{Q}_s = DNI * \eta_{optical} * \eta_{other} * A_a \quad (4.3)$$

$$(1 - \alpha) * \dot{Q}_s = \sigma * \epsilon_r * \sum_{i=1}^n A_i * F_i * (T_{ri}^4 - T_a^4) + h * A_r * (\bar{T}_r - T_a) + \dot{Q}_{out} \quad (4.4)$$

Figure 4.1.6 shows the energy balance of the external receiver. Multiple heat transfer mechanisms are shown: incident radiation component (\dot{Q}_s), convection component (\dot{Q}_{conv}), radiation component (\dot{Q}_{rad}) and reflection component (\dot{Q}_{ref}).

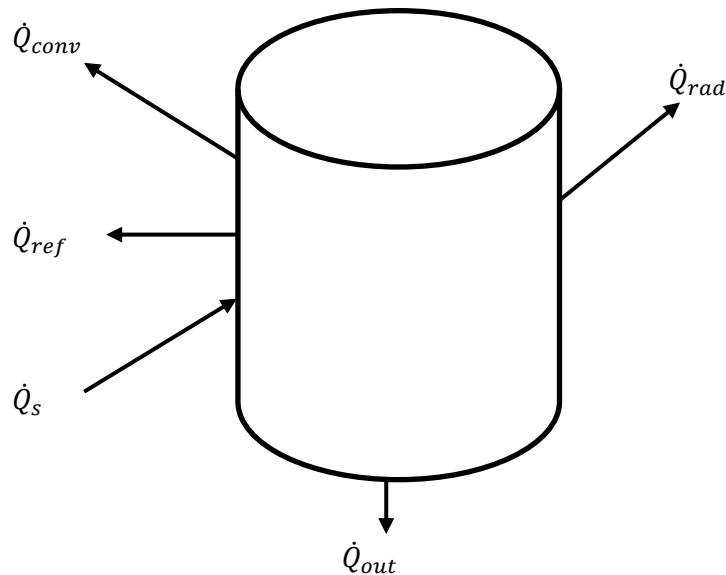


Figure 4.1.6: External receiver energy balance

4.1.7 Thermal Storage System Operating Parameters

The thermal energy from the receiver is sent to the TES and then transferred to the steam loop when needed (for example during peak demand time). Commercially available TES show a round trip efficiency of 95 % (Denholm & Mehos 2011), resulting in an average loss of 5 % per 24 hours or 0.2 % per hour. The model for this study assumed a 90 % round trip efficiency for the TES. This led to an average loss of 10 % per 24 hours or 0.5 % per hour. The study model was more conservative in the sense that it assumed more losses than is recorded for commercially available TES; this should be looked at in future.

4.1.8 Power Block

No specific turbine was selected for this study, but a theoretical Chambadal-Novikov (c-n) efficiency was used to determine the performance of the steam turbine (Novikov 1957). The Chambadal-Novikov efficiency represents the utility plants well. Table 4.1 shows the power plant efficiency. The actual efficiency of the Gemasolar plant is 40 %. When considering the high and low temperature reservoir and applying Chambadal-Novikov efficiency, the result is 40.3 %. The high temperature reservoir is the hot salt temperature, and the low temperature reservoir is the ambient temperature, assuming dry cooling is used. The model assumes dry cooling, and this is based on the South African conditions, which require conservative water consumption. However, careful consideration of adapting dry cooling is needed in order to understand that the performance trade-off is decreased efficiency. The following method was used to determine the efficiency of the heat engine and the work done.

The Carnot efficiency represents an ideal efficiency of the heat engine (but is not achieved in practice). The Carnot efficiency indicates the upper limit of efficiency and is always higher than the actual efficiency. It is an internally reversible process and operates between the hot reservoir, T_H , and the cold reservoir, T_L . The equation (4.5) shows the Carnot efficiency equation.

$$\eta_{th} = 1 - \frac{Temp_{low}}{Temp_{high}} \quad (4.5)$$

$$\eta_{th} = 1 - \sqrt{\frac{Temp_{low}}{Temp_{high}}} \quad (4.6)$$

Table 4.1 shows the actual efficiencies of the two CSP plants along with comparisons for the actual efficiency with the Carnot efficiency and Chambadal-Novikov efficiency. While using the Gemasolar plant as reference, it is indifferent to the exact power block used. The equation (4.6) shows the Chambadal-Novikov efficiency equation.

Table 4.1: Chambadal-Novikov efficiency and actual efficiency comparison

| Power Plant | T_{low} [°C] | T_{high} [°C] | η_{carnot} [%] | $\eta_{chambadal-novikov}$ [%] | η_{actual} [%] |
|--------------------|-------------------|--------------------|------------------------|-----------------------------------|------------------------|
| Gemasolar | 25 | 565 | 64.4 | 40.3 | 40 |
| Solar Two | 25 | 540 | 63.3 | 39.4 | 34.1 |

$$\dot{W} = \eta_{th} * \dot{Q}_{pb} \quad (4.7)$$

The equation (4.7) is used to determine the power by calculating the efficiency conversion of thermal energy in the working fluid that is sent to the turbine.

4.1.9 Parasitic Power

The parasitic power consumption in a CSP plant generally is comprised of the auxiliary equipment energy requirements and the control room energy requirements. These requirements are a small fraction of the total gross output of the plant. The parasitic losses for the Gemasolar plant were not available for use on this model. Instead, parasitic losses of 5 % of the total gross output were assumed.

4.1.10 Power Plant Scaling

The CSP system is comprised of three independent yet interrelated primary components. These components can be sized for optimal operation of the CSP plant:

- The solar field, which collects the solar radiation and produces the thermal energy.
- The TES system, which stores the thermal energy in the HTF.
- The turbine, which converts the thermal energy and mechanically transfers that energy into the electricity generator.

The specified component sizes and operating parameters for the Gemasolar plant are 20 MW turbine with 15 hours storage TES and a solar field. In order to achieve the adequate capacity that meets the assumed peak load demand, these parameters were scaled up or down assuming that it is valid to do so. An illustration of the scaling of the CSP primary components is shown in Appendix B.

Fulfilment and Curtailment

- Fulfilment is a scenario where the CSP is able to deliver the assumed electricity load demand at that particular time.
- The curtailment refers to the scenario where, for various reasons, the CSP does not utilize some of its energy by intentionally releasing or dumping the energy. However, all these reasons require the CSP plant not to deliver energy to the grid at that particular time. This can also be done by defocusing some of the mirrors because the solar field is producing more energy than the TES can accommodate.

Solar Field

The solar field multiple³ is used to achieve the adequate solar field capacity in any site. The solar field multiple determines the number of solar fields that are equivalent in size to those at Gemasolar plant. The two factors that influence determining these parameters are the fulfilment coefficient and the curtailment coefficient. The solar field and the tower are fixed with the Gemasolar plant specification. This means that irrespective of the turbine size and the storage size, the solar field will collect the same amount of energy. The field and tower scale together or multiply to keep the assumption of scaling valid. It does not matter if it is big or if it is a multiple of plants.

Turbine

The turbine rating is set at any value. Scaling up or down of the turbine affects the fulfilment and curtailment coefficients. Ideally, for a peaking CSP plant, the installed turbine will be big relative to the TES capacity. This allows for a quicker discharge of the stored energy during the peak period. The turbine rating that was specified in this model is optimised for the determined peak load demand.

Thermal Storage System

The TES is specified by full hours to the turbine, which implies that it scales automatically with the turbine.

³ Solar field multiple refers to the scaling factor used to scale up or down the solar field. The same multiple is used to scale the TES and the Turbine in order to keep the assumption of scaling valid. It should not be confused with the “solar multiple” which defines the capacity of the solar field over the turbine rating.

If it is to remain the same size and the turbine multiplied, the operational hours of TES are reduced. If it remains the same size and the turbine reduced, then the operational hours of the TES are increased.

Figure 4.1.7 illustrates the scaling relationship between turbine and TES when the solar field is held constant. The graph is based on the Gemasolar plant component sizes. When the TES hours are decreased, the turbine rating is increased, as is desirable for the peaking CSP plant. It is predicted that a bigger turbine with fewer storage operational hours would be ideal for a peaking CSP plant.

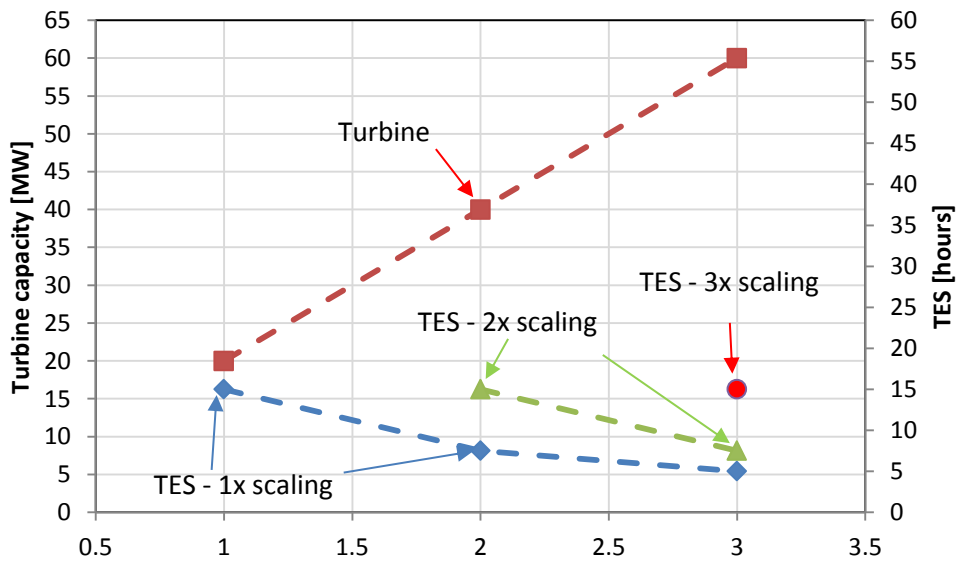


Figure 4.1.7: CSP system components scaling

4.2 OCGT Plant Model

The OCGT technical model that was developed for this study is based on the current OCGT systems that are operated by Eskom. An OCGT plant has an efficiency of 35 % (Brinckerhoff 2008). It allows for a quick ramping to follow the load demand, thus simple for hour model.

4.3 Conclusion

The technical model chapter shows the two technical models that are used for this study – the CSP and OCGT technical model. The CSP technical model is an optical to thermal energy model. The OCGT technical model is based on the current OCGT efficiency. This chapter revealed that these technical models that are used in this study are suitable to determine the objective of this study. The models are simple enough to factor the operational parameters of the two technologies and quick to produce instantaneous results.

5 Scenario Modelling

To determine the feasibility of utilising the CSP systems in this study, the LCOE of the CSP was compared with the LCOE of the OCGT system. The main aim for comparing the two systems was to obtain the optimum LCOE of the CSP and OCGT respectively. The three scenarios modelled in this study are:

- The business as usual scenario: OCGT energy supply
- CSP scenario: grid energy backup
- The combined systems scenario: CSP system coupled with OCGT system

The first scenario is the OCGT system energy supply analysis. This scenario analysed the current peaking energy system in South Africa, whereby the OCGT is used to supply the peak energy demand. Currently, OCGT systems are utilized as peaking stations in South Africa. This system provides base case for comparison with the other scenario.

The second scenario is the utilization of a CSP system as the only peaking system. In this scenario, grid energy is used during the days when there is not enough solar resource. The grid energy is only used to meet the gap demand that the CSP system is unable to meet. The grid electricity is used, when it can, to charge the storage tank.

The third scenario is a CSP system that is coupled with the OCGT system. The OCGT system is only used to meet the gap demand that the CSP system is unable to meet. The LCOE results from the CSP system scenarios were compared with the OCGT system LCOE. This section discusses and presents the different scenarios of peaking systems in South Africa.

5.1 Business as Usual Scenario: OCGT Energy Supply

The first scenario is referred to as the 'business as usual scenario'. It predicts that the OCGT system will continue to be used as key peaking stations in South Africa. This scenario assumes that the proposed OCGT capacity is installed to produce peak energy as defined in the IRP. The OCGT technology is characterized by low capital costs and high O&M costs. These systems can be installed in short lead time and have very low weight density. They can also be easily installed in modular form. OCGT systems provide a very good operation due to their ability to be electronically controlled. The records show that they can be brought on line and synchronised with the grid in about 10 minutes. During the time when they are not generating power, they are synchronised with the grid by using parasitic power. The parasitic power that is needed for the OCGT system is about 2 – 5 % of the installed capacity (Eskom 2010a).

The analysis of the OCGT system considered the technical operation and the financial model of the system. The technical operating parameters were adapted from the specification of the Eskom operated OCGT system (Eskom 2009). Also, the financial model input parameters for the capital expenditure were obtained from the OCGT systems' cost estimates report (Brinckerhoff 2008). Table 5.1 provides the operating parameters and the capital expenditure information for the OCGT systems that are currently utilized in South Africa.

Table 5.1: OCGT costs breakdown (Brinckerhoff 2008)

| Item | Value | Unit |
|------------------------|--------|---------------|
| Plant costs | 593.28 | US\$/kW |
| Fixed O&M | 10.35 | US\$/kW/annum |
| Variable O&M | 0.0065 | US\$/kWh |
| Fuel energy value | 35 | MJ/kg |
| Density diesel | 0.832 | kg/l |
| Gas turbine efficiency | 0.35 | |
| Diesel costs | 9.89 | ZAR/kg |
| Diesel costs | 11.89 | ZAR/l |

5.1.1 OCGT Analysis of LCOE

The capacity uptake for the OCGT was utilized to meet the peak load demand that was assumed for this study. Table 5.2 provides information about the proposed OCGT capacity for this model. During implementation, the proposed capacity will not be implemented homogenously but would have an incremental uptake over the years. However, the theoretical model that was developed for this study assumed that the whole capacity is available homogenously to meet the assumed peak load demand, and the analysis was conducted based on that capacity.

The cost analysis of the OCGT system was based on the theoretical costs. The LCOE model assumed 8 % interest rate on the loan and 10 % discount rate. The assumed lifetime of the energy system was 30 years.

The OCGT system generates the total assumed peak load demand. Due to the operational flexibility of the system, it has a fulfilment of 1.0, assuming capacity is always available. The energy costs and the LCOE costs were used as inputs to determine the LCOE of the system. The LCOE of the OCGT system in this scenario is 5.08 ZAR/kWh for the assumed energy demand of 7 587.44 TWh.

Table 5.2: OCGT capital and O&M costs (Brinckerhoff 2008)

| Item | Total |
|----------------|---------------------|
| Plant capacity | 5 000.00 [MW] |
| Plant costs | 2 966.37 [Mio US\$] |
| Fixed O&M | 51.75 [Mio US\$] |
| Variable O&M | 45.76 [Mio US\$] |
| Total O&M | 97.51[Mio US\$] |

5.1.2 Fuel Sensitivity Study

The IRP states that the future peak load will be met by the OCGT systems in South Africa (DoE 2011). It further states that these systems will be run on diesel in the short-term. This is based on the established infrastructure of the diesel supply chain in South Africa. Running the OCGT systems on natural gas will be beneficial because it could result in lower LCOE. The IRP also points this out as a long-term target, acknowledging that natural gas is cheaper than diesel, and it would make business sense to use it (DoE 2011). Currently, natural gas supplies about 3 % of the energy demand in South Africa (Moolman 2013). Establishing well known natural gas reserves and the supply chain infrastructure is a long-term target. In this study, diesel fuel was used as the energy source for running the OCGT in the short-term.

Over the past few years, fossil fuel prices, including diesel prices, have fluctuated significantly. Fluctuations in diesel prices will significantly impact the energy costs of OCGT systems. Figure 5.1.1 shows the lifetime costs of the OCGT plant. It shows that the fuel costs make up a significant amount of the total costs.

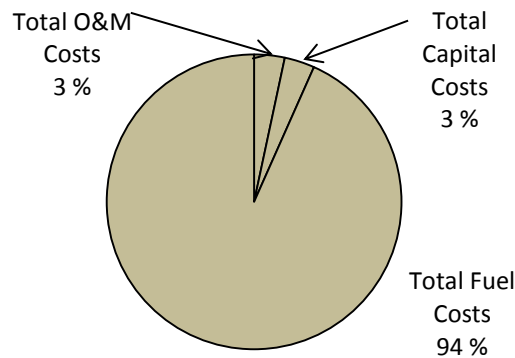


Figure 5.1.1: Lifetime costs of OCGT system

Figure 5.1.2 shows the sensitivity analysis of the OCGT system to fuel costs. The graph indicates the LCOE under different conditions, which shows the annual increase in fuel costs will range between 0 % and 10 %. This shows the sensitivity analysis to fuel inflation and does not assume that this is the range.

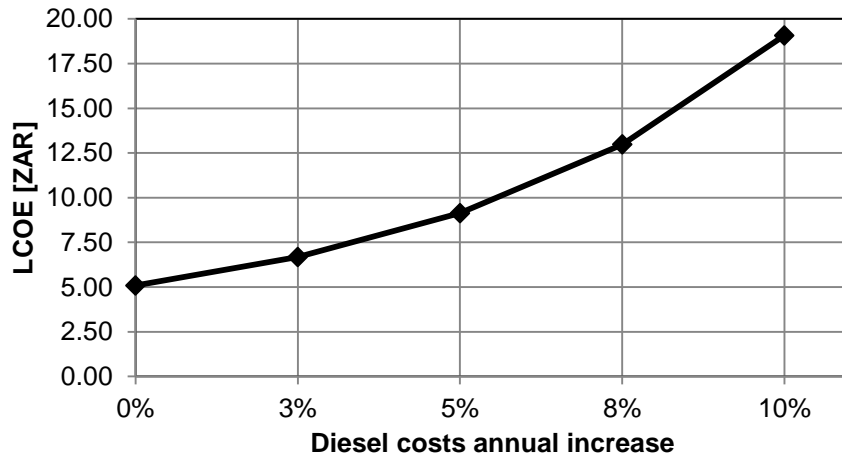


Figure 5.1.2: OCGT system LCOE fuel sensitivity analysis

5.2 CSP System Description

The second scenario is the utilization of a CSP system as a peaking system. Different CSP central receiver plants were located in different proposed sites along the high capacity line. The proposed CSP capacity delivered the assumed energy demand, as shown in Figure 3.1.2a and 3.1.2b, which is the same for the OCGT system.

Table 5.3: CSP system configuration

| CSP plants | Solar Field [m ²] | TES [MWh] (hours) | Site capacity [MW] | Receiver/ Turbine ratio |
|------------|-------------------------------|-------------------|--------------------|-------------------------|
| Gemasolar | 304 750 | 148 (15) | 20 | 6 |
| Site 1 | 1 590 000 | 1 217 (7) | 350 | 3 |
| Site 2 | 1 590 000 | 1 217 (7) | 350 | 3 |
| Site 3 | 1 590 000 | 1 043 (7) | 300 | 3 |
| Site 4 | 1 590 000 | 1 217 (7) | 350 | 3 |
| Site 5 | 1 590 000 | 1 217 (7) | 350 | 3 |
| Site 6 | 1 590 000 | 1 217 (7) | 350 | 3 |
| Site 7 | 1 590 000 | 1 217 (7) | 350 | 3 |
| Site 8 | 1 590 000 | 1 043 (7) | 300 | 3 |
| Site 9 | 1 590 000 | 1 043 (7) | 300 | 3 |
| Site 10 | 1 590 000 | 1 043 (7) | 300 | 3 |

Table 5.3 shows the capacity of the CSP primary components from the 10 proposed sites. It shows the total solar field, total TES capacity and total site capacity from each site.

The solar resource data – DNI that was used for this study is a Typical Meteorological Year (TMY) data and was supplied by GeoModel solar. It is derived from hourly time series. Figure 5.2.1 shows the annual sum of the DNI from the 10 sites.

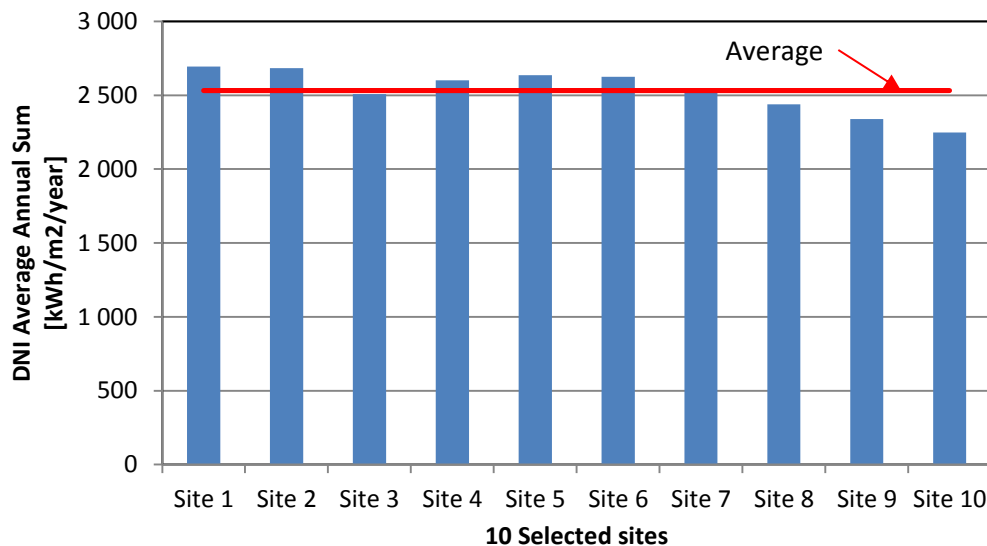


Figure 5.2.1: Annual average sum of DNI from 10 selected sites Data: (Geomodel Solar 2012)

5.3 Scenario 2 – CSP + Grid Electricity Thermal Energy Supply

This scenario considered the technical and financial feasibility of the CSP systems operation as the peaking station. The technical feasibility looked at the ability of the CSP system to deliver the assumed peak load demand.

The TES plays a big role in the operation of the proposed peaking CSP system. Thermal energy is sent to the TES during off-peak periods and sent to the turbine from the TES during peak periods. Figure 5.3.1 shows two days of the CSP system operation – energy delivery of the entire CSP system network from all the proposed sites. On the second day, the CSP system does not fulfil the energy demand. This is based on the inadequate solar resource and the limitations of installed capacity of the CSP system. While the CSP system could achieve a fulfilment 1.0, it is optimised for the LCOE, meaning that the storage can be made bigger in order to supply the gap demand. However, a bigger storage will result in a higher LCOE.

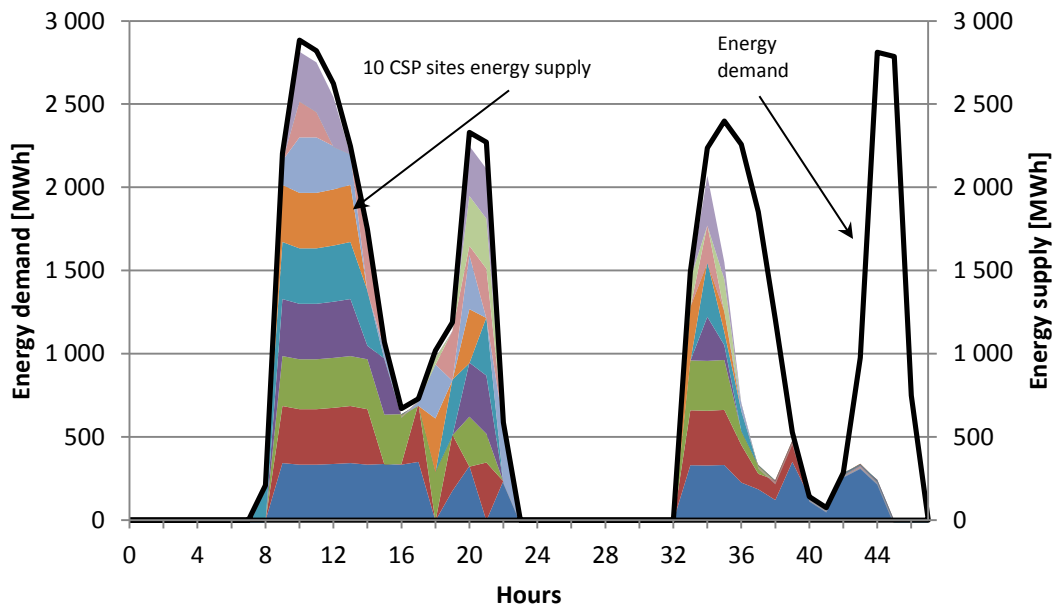


Figure 5.3.1: CSP system operation configuration

5.3.1 CSP System LCOE Study

The energy output from the CSP system was used as an input parameter in the financial model. The financial model requires capital expenditure costs of the CSP system. For this study, no actual costs of an operational CSP plant were available. The capital costs are theoretical estimates. All the figures in Table 5.4 for the capital costs estimates were obtained from the Sandia report of CSP components cost estimation (Kolb et al. 2011). These capital costs of the CSP system are estimates that are stated in the SANDIA power technology roadmap (Kolb et al. 2011). The costs are based on the baseline tower system with 100 MW and 9 hours of storage and the solar field with 1 000 000 m².

Table 5.4 shows the capital costs of the proposed CSP system, which were inputs to the LCOE model. The LCOE financial model assumed an 8 % interest rate on the loan and 10 % discount rate. The assumed lifetime of the energy systems was 30 years. The results of the CSP system modelling showed that the CSP performs well as a peaking system. This performance was determined by the amount of energy that the CSP system was able to deliver and the LCOE of the CSP system. Apart from the LCOE, the fulfilment and the curtailment were the key aspects of the CSP scenario analysis.

Table 5.4: CSP system capital and O&M costs (Kolb et al. 2011)

| Item | Value [\$] | Unit | Total costs [Mio \$] |
|------------------|------------|----------------------|----------------------|
| Capacity | 3 300 | MW | |
| Optical | 200.00 | \$/m ² | 3 180.00 |
| Receiver | 200.00 | \$/kW _{th} | 1 200.00 |
| Storage | 30.00 | \$/kWh _{th} | 1 721.69 |
| Power plant | 1 000.00 | \$/kW _e | 3 300.00 |
| Steam gen | 350.00 | \$/kW _e | 1 155.00 |
| Sub total | | | 10 556.00 |
| Balance of plant | 0.15 | | 1 583.50 |
| Total | | | 12 140.19 |
| O&M | 65.00 | \$/kW _{yr} | 214.50 |

The CSP components in Table 5.4 have been grouped together into primary components. Other reports on CSP systems costs breakdown will have the heliostats separated from the site preparation. However, this report combined the related costs of each component. The engineering and site preparations are included in the solar field costs. The tower costs are included in the receiver costs, and the balance of plant costs are included in the power block costs (Kolb et al. 2011). An average of 15 % for contingencies was used for this study (Kolb et al. 2011). Table 5.5 shows the amount of energy delivered by the CSP system.

Table 5.5: CSP delivered peak energy

| Item | Value | Unit |
|----------------------------------|--------------|------|
| National Peak energy demand | 7 587 443.16 | MWh |
| CSP system peak energy delivered | 6 988 151.77 | MWh |

Table 5.6 shows the LCOE of the CSP plant along with the fulfilment and the curtailment coefficients of the CSP system.

Table 5.6: CSP system LCOE results

| Item | Value | Unit |
|-------------------------|-------|---------|
| LCOE | 1.89 | ZAR/kWh |
| Fulfilment coefficient | 0.82 | |
| Curtailment coefficient | 0.06 | |

Curtailment

The model in this study is optimised to deliver energy during peak periods. During the course of the day when there is high solar resource, the thermal energy from the receiver is only sent to the TES. If the TES system gets fully charged, this excess energy is regarded as curtailed. The curtailment energy that is indicated here is a result of a scenario when the storage is full. This excess electricity can be sold to the grid but this model is conservative.

Figure 5.3.2 shows the storage charge level and the curtailment energy for three days for a random CSP system site. The combination of all sites will conform to the same phenomenon with regards to the curtailment – see Appendix C.

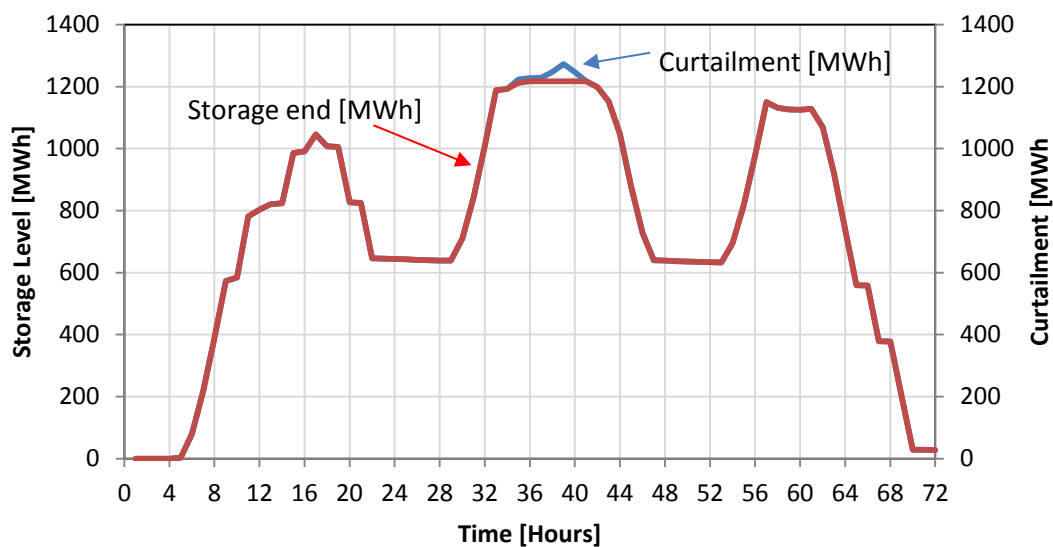


Figure 5.3.2: Storage charge level and energy curtailment – random site

Curtailment coefficient – curtailment occurs due to supply exceeding demand. The demand is defined strictly in this study but it would be reasonable to assume that excess energy could be sold in off-peak periods to further improve cost performance of the system. Curtailment is only significant when the complete CSP system is deployed. A CSP system optimised for this purpose but not fully commissioned will tend to deliver all electricity produced.

Fulfilment

The fulfilment refers to the ratio of the CSP system delivered energy to the assumed load demand. The CSP system has a fulfilment coefficient of 0.82 – fulfils 82 % of the assumed load demand. This is based on the fact that the optimal LCOE of the CSP system is achieved at this fulfilment coefficient. In order to fulfil the full peak load demand, other sources will be required.

5.3.2 Grid Energy Supply Analysis

The main idea for utilizing the grid energy with the CSP system would be to guarantee the energy during the peak period. In such a case, the TES system would be connected to the grid when the CSP plant is operating. This would allow energy to be purchased from the national grid during periods of low demand and energy to be fed back into the grid during periods of high demand. During periods when there is not enough energy supplied from the solar field, for instance due to bad weather, the storage tank would be charged by the grid energy. Energy would be purchased from the grid, stored in the TES system and then sent to the grid during peak load demand.

Figure 5.3.3 shows the layout of the CSP plant in this configuration. The purchased energy is used to heat the cold salt from the cold tank to hot tank through a special loop. The special loop is used to limit the energy requirements that would be needed to pump cold salt through the tower.

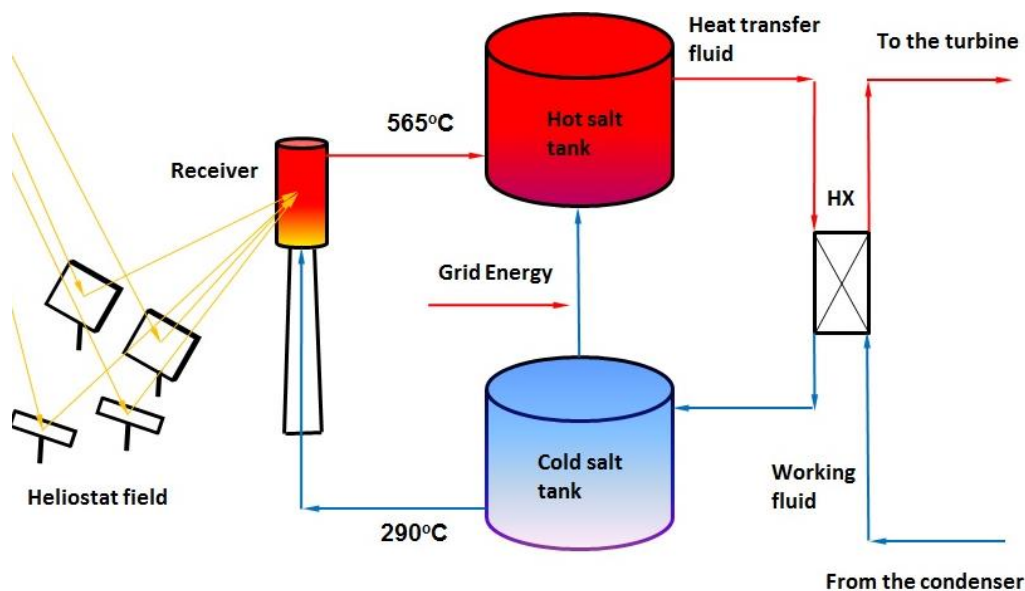


Figure 5.3.3: TES grid energy purchase

When the energy is brought to the TES system from the grid, it is subjected to thermal losses. The energy in the storage is sent to the steam generator to generate steam that is used to turn the turbine. The Chambadal-Novikov is used to estimate the amount of purchased electricity that can potentially be sent back to the grid. Table 5.7 lists the losses considered during the purchase of the energy.

While converting electricity to thermal energy in the salt tank and converting that thermal energy to electricity, as proposed in this project, it does not make pure technical sense due to high losses but economics might work.

Table 5.7: TES thermal losses efficiency

| Component | Efficiency |
|------------------------------|------------------------------|
| Turbine efficiency | Chambadal-Novikov efficiency |
| TES system charge efficiency | 98 % |
| TES system thermal losses | 98 % per hour |

5.3.3 Eskom Flexi Rates

The energy bought from the grid was based on weather predictions. In order to predict the grid energy purchase for this study, a proxy weather model was developed. The available DNI solar resource used in this model was also used to develop the proxy weather prediction. Random numbers from Microsoft Excel were used to create a different DNI profile. Each run of random numbers creates a different new DNI profile. Figure D1 – in Appendix D shows the actual DNI used on the model and the randomised DNI for the same day. The new DNI profile was then used to forecast the weather and thus determine the energy purchase. The grid energy was purchased during off-peak periods and sent to the grid during peak periods. Since national demand and energy tariffs are lower during off-peak periods, this method of energy purchasing might make economic sense. Table 5.8 shows the tariff structure that was used for electricity purchase.

Table 5.8: Eskom RURAFLEX tariffs (Eskom 2012b)

| Active Energy Charge [c/kWh] | | | | | |
|--------------------------------|----------|----------|-------------------------------|----------|----------|
| High demand season [Jun – Aug] | | | Low demand season [Sep – May] | | |
| Peak | Standard | Off-peak | Peak | Standard | Off-peak |
| 360.70 | 92.47 | 48.66 | 99.35 | 60.20 | 41.63 |

When the proxy weather model predicted inadequate solar resource for the next day, the required amount of energy was (theoretically) brought from the grid to charge the hot tank. This grid energy factors in the modified Carnot efficiency losses, the TES charge losses and the TES hourly thermal losses.

5.3.4 National Load Demand Increase

Purchasing energy during off-peak periods resulted in a new national load demand profile. Figure 5.3.4 shows the two days of national load demand: the previous load demand before the energy purchase for the CSP system and the new electricity demand caused by the energy purchase for the CSP system. On the first day there was a substantial amount of energy needed to charge the TES. The average increase in energy demand based on the energy purchase was 4 % annually.

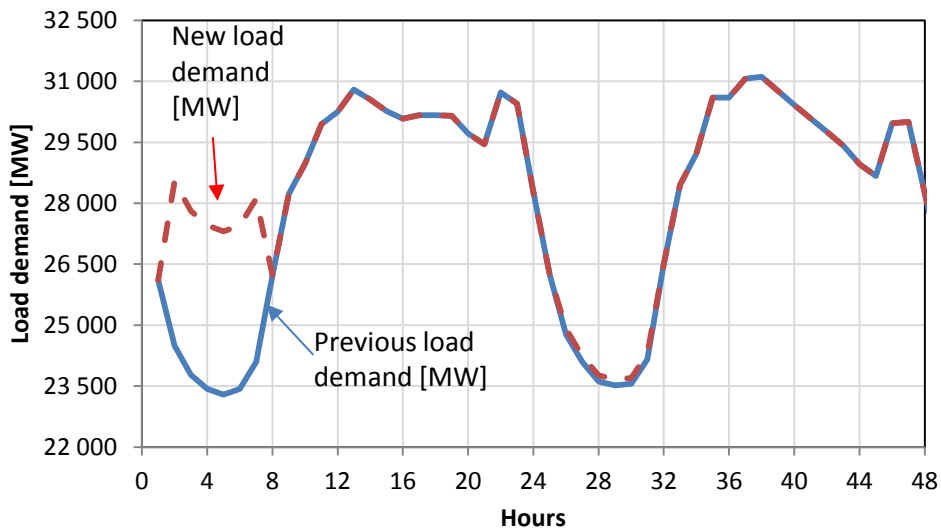


Figure 5.3.4: National electricity demand load profile increase

5.3.5 Grid Electricity Purchase Guarantee

Ideally, the energy purchase from the grid should be equal to the required electricity demand gap, but in reality purchased electricity is always more or less than the actual demand. This is because the purchase of grid electricity is based on the weather prediction, and the demand cannot be predicted. Figure 5.3.5 shows the fulfilment coefficient of the electricity demand gap only. It also shows the forecast purchase coefficient – the ratio of the amount of purchased electricity and the electricity demand gap. The ideal situation is to purchase the same amount of electricity that is required and still achieve a fulfilment of 1.0. However, achieving that has cost implications. As the forecast purchase coefficient increases, the fulfilment coefficient stabilises. The purchased electricity amount doubles the electricity demand gap amount and still the purchased electricity does not fulfil the electricity demand gap.

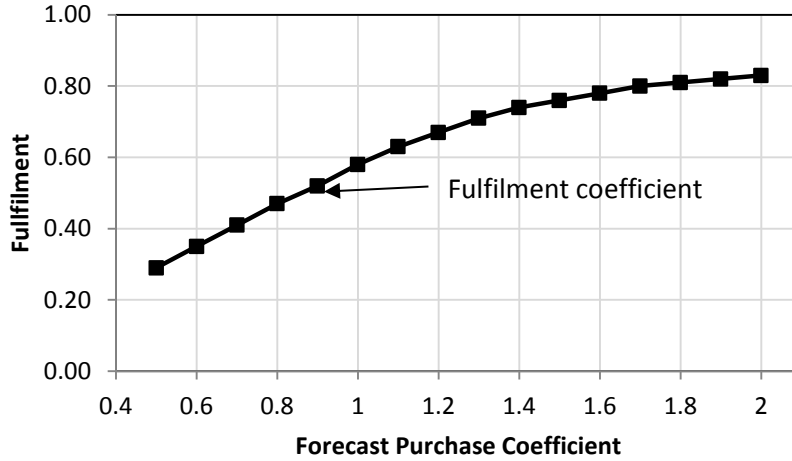


Figure 5.3.5: Grid electricity purchase fulfilment analysis.

To remain conservative, the forecast purchase coefficient of 1.0 is assumed for the grid electricity purchase. Table 5.9 shows the amount of electricity demand gap, electricity purchased from the grid and the fulfilment coefficient of the electricity demand gap. The energy that was purchased from the grid fulfilled 59 % of the electricity demand gap.

Table 5.9: Grid energy purchase results

| Item | Value | Unit |
|--------------------------------|--------------|------|
| Energy demand (gap demand) | 1 348 741.72 | MWh |
| Energy delivered (grid energy) | 792 164.96 | MWh |
| Fulfilment | 0.59 | |

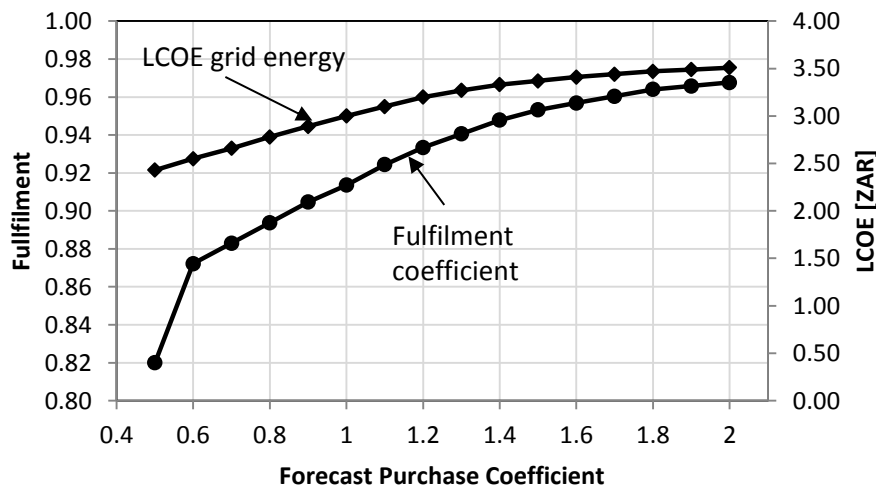


Figure 5.3.6: CSP system + grid electricity fulfilment analysis

The energy that was purchased from the grid was combined with the energy that was generated by the CSP to determine the total LCOE of the system. Figure 5.3.6 shows the total LCOE and the total fulfilment of the CSP system and grid electricity. Initially, the CSP system energy supply had a fulfilment of 0.81. Using the grid electricity seeks to achieve a fulfilment of 1.0, but achieving that has cost implications. As the forecast purchase coefficient increases, the fulfilment levels off. The results of the combined system LCOE are shown in Table 5.10. The coupling of the CSP system with the grid energy resulted in a 47.6 % increase in LCOE from 1.89 ZAR/kWh to 3.00 ZAR/kWh. Utilizing grid energy increased the fulfilment coefficient of the CSP system from 0.82 to 0.92, using a forecast purchase coefficient of 1.0. A system increasing fulfilment to 1.0 would be more expensive but this has not been fully explored.

Table 5.10: Combined CSP and grid energy results

| Item | Value | Unit |
|--------------------------|--------------|-------------|
| LCOE | 3.00 | ZAR/kWh |
| Energy generated (CSP) | 6 238 701.44 | MWh |
| Energy demand (total) | 7 587 443.16 | MWh |
| Energy generated (total) | 7 030 866.40 | MWh |
| Fulfilment total | 0.92 | |

5.4 Scenario 3 – Combined CSP System and OCGT System

This combined scenario utilized the CSP system in combination with the OCGT system to construct a hybrid system that could efficiently and effectively respond to peak energy demand. This scenario assumed that both the proposed capacity of the CSP and the proposed OCGT capacity would be implemented. However, only the CSP capacity was utilized to meet the predetermined peak load demand, while the OCGT was only utilized to guarantee meeting demand.

Table 5.11: CSP system and OCGT proposed capacity

| Item | Value | Unit |
|-------------|--------------|-------------|
| CSP system | 3 300 | MW |
| OCGT system | 5 000 | MW |

Table 5.11 indicates the proposed capacities of the CSP and the OCGT systems, showing each technology has a substantial amount of capacity to meet the assumed load demand. Only the CSP system is utilized at full capacity to meet the load demand. The OCGT is underutilized because it generates only a small amount of energy to cover the gap demand.

Figure 5.4.1 shows the operation of the CSP and the OCGT system over a two day period (February). The CSP system fulfils the demand on the first day but not on the second day. As the Figure indicates, the CSP system delivers energy at its full capacity whenever there is adequate solar thermal energy and the OCGT delivers the demand gap implying that the OCGT system delivers a smaller amount of energy relative to installed capacity.

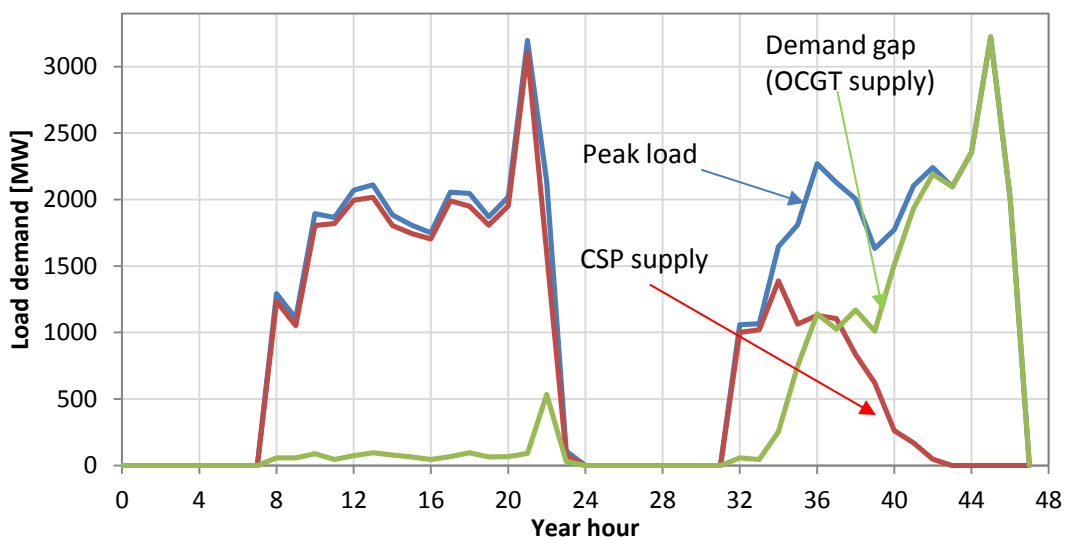


Figure 5.4.1: CSP system operation configuration

5.4.1 LCOE CSP System

Table 5.12: CSP energy delivered and the LCOE

| Item | Value | Unit |
|--------------------------|--------------|---------|
| LCOE of the CSP | 1.89 | ZAR/kWh |
| Energy generated | 6 238 701.44 | MWh |
| Fulfilment coefficient | 0.82 | |
| Curtailement coefficient | 0.06 | |

The CSP system operation was the same as the previous section, as was the proposed capacity and assumed peak load demand for this scenario. The LCOE of the CSP also remained the same as described in the previous section, and the CSP system supplied the same amount of energy as when coupled with the grid energy supply. Table 5.12 shows the LCOE of the CSP and the amount of energy from the CSP, as well as the fulfilment and the curtailment of the CSP.

5.4.2 LCOE OCGT System

The OCGT system was linked with the CSP system and was only used to supply the gap energy demand; consequently, a limited capacity of the OCGT system was utilized. This resulted in a low capacity factor for the OCGT system. The underutilization of the OCGT system resulted in high LCOE costs of the OCGT, and the capital costs as well as O&M costs were high relative to the energy generated by the system. The implications of the lower capacity factor were higher LCOE. The first scenario presented the operation of the OCGT as a peaking station. The LCOE of the OCGT scenario when the OCGT generated all the peak load energy was 5.08 ZAR/kWh. However, when the OCGT was used to supply the gap energy, the LCOE was high. Table 5.13 details the LCOE of the OCGT and the amount of energy generated.

Table 5.13: OCGT energy delivered and the LCOE

| Item | Value | Unit |
|------------------|--------------|---------|
| LCOE of the OCGT | 6.77 | ZAR/kWh |
| Energy generated | 1 348 741.72 | MWh |

5.4.3 OCGT LCOE Fuel Sensitivity Analysis

The financial model of the OCGT was based on current conditions. Increases in fuel prices affect the LCOE. Figure 5.4.2 shows the LCOE fuel sensitivity of the OCGT system when the OCGT was used alone and when it was used to supply the energy demand gap, scenarios 1 and 3 respectively. The increase in fuel prices resulted in increasing LCOE of the OCGT.

5.4.4 Combined LCOE

The fuel sensitivity analysis of the OCGT showed that increases in fuel prices result in increases in LCOE. The CSP system performed well when coupled with the OCGT system, and it cushioned the high LCOE of the OCGT because the operational costs of the CSP were low and the LCOE was constant. On the other hand, the OCGT has high operational costs. Figure 5.4.2 shows the fuel sensitivity analysis of the OCGT system and how it performed when coupled with the CSP.

The graph illustrates that the LCOE of the OCGT system substantially increased due to the fluctuating fuel costs; however, the combined LCOE was brought down by coupling the OCGT with CSP

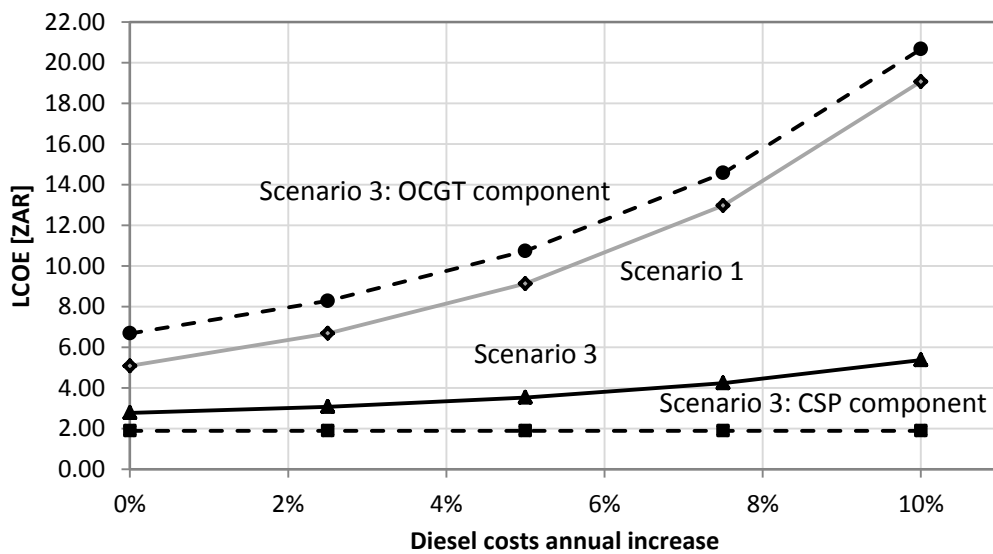


Figure 5.4.2: Combined LCOE of OCGT and CSP

Table 5.14 shows the combined LCOE of the CSP and OCGT systems. The LCOE of the CSP is 1.89 ZAR/kWh when the system operates alone. When linked with the OCGT as a virtual hybrid system, the combined LCOE is increased by 31.2 %. The LCOE of the OCGT when operating alone is 5.08 ZAR/kWh. When it is linked with the CSP, the combined LCOE is decreased by 44.4 %.

Table 5.14: CSP combined with OCGT LCOE

| Item | Value | Unit |
|------------------|--------------|---------|
| LCOE total | 2.78 | ZAR/kWh |
| Energy generated | 7 587 443.16 | MWh |

5.5 Conclusion

This chapter presented three scenarios of the peaking systems in SA. The OCGT system scenario shows that the OCGT systems generate energy in excess of 5.08 ZAR/kWh. Further, this scenario shows that the OCGT systems are vulnerable to fluctuating diesel prices. The CSP scenario established that the CSP systems generate the peak energy at 1.89 ZAR/kWh. The utilization of grid electricity by CSP systems to supply the gap energy demand results in LCOE increase of 37 %. The scenario that combines the CSP system and the OCGT system results in a combined LCOE of 2.78 ZAR/kWh. This scenario results in the lowest LCOE and it guarantees electricity generation.

6 Implementation Proposal

This chapter presents the envisaged CSP system implementation proposal. The aim is to identify the most appropriate method of implementing the proposed CSP system capacity and determine how the implementation affects the LCOE, fulfilment and curtailment. The subsequent section discusses the Geographic Information Systems (GIS) study, which examines the availability of suitable land for developing CSP plants on the proposed sites.

6.1 Implementation Plan Costs Analysis

The theoretical model demonstrated the total capacity of the CSP system. This study assumed the homogenous availability of all the proposed CSP capacity. Realistically, however, this capacity will be implemented in incremental phases, as the small CSP capacity will be constructed in a rollout model. When considering the high capital costs and the modularity of CSP, this progressive model is most suitable. It was further assumed that the progressive rollout model will assist in finance, by using the energy cost savings from the implemented CSP plant to implement the next CSP plant.

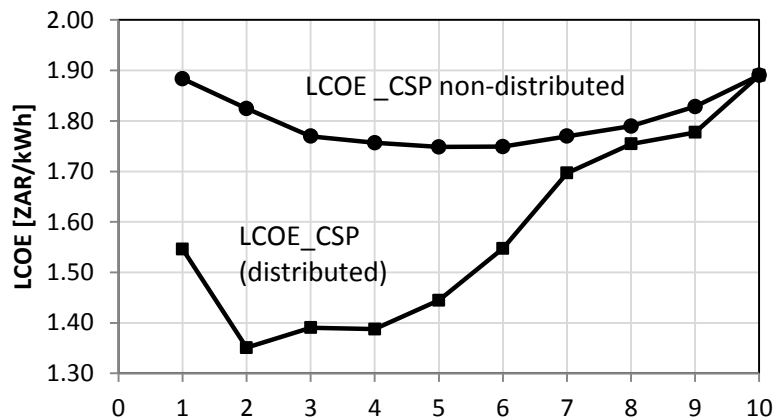


Figure 6.1.1: Implementation proposal LCOE sensitivity analysis

LCOE

The LCOE of the CSP system was optimised for the total proposed CSP capacity. This was done by modelling the total proposed capacity and the assumed peak load demand to obtain the optimised LCOE. The incremental implementation of the CSP plants requires optimisation to obtain the highest LCOE during each capacity construction. Optimization of LCOE during incremental uptake was not done for this study. This study analysed the implications of non-distributed and distributed uptake of the CSP plants based on the proposed capacity.

Figure 6.1.1 shows the LCOE sensitivity of the distributed uptake and the non-distributed uptake. The distributed CSP capacity uptake means that the proposed capacity on site 1 is implemented, and implementation is done to the next sites consecutively. The non-distributed capacity uptake means that a small percentage of the proposed capacity from each site is implemented at the same time. The distributed CSP implementation phasing option performs better than the non-distributed implementation. During the phasing implementation, the LCOE of the distributed CSP is lower than the LCOE of the no-distributed CSP.

Fulfilment

During the implementation of the CSP plants, the fulfilment started slowly and increased as the capacity uptake increased. The fulfilment coefficient also increased as the CSP capacity increased until the total proposed capacity was installed. The distribution of CSP plants during the incremental uptake has advantages for the performance of the CSP system. Figure 6.1.2 shows the implications of the distributed and non-distributed capacity uptake of the fulfilment coefficient.

The distributed capacity had a higher fulfilment coefficient than the non-distributed capacity. During the non-distributed uptake, the proposed capacity in each proposed CSP site was installed. The second site proposed capacity was installed after the previous capacity uptake. On the distributed uptake, a small capacity was installed on many sites at the same time. The distributed uptake performed better than the non-distributed uptake. When bad weather occurred, specifically over the small non-distributed CSP plant, it affected the energy output from the plant. However, if the CSP plants were distributed, the bad weather did not affect all the CSP plants in the different sites.

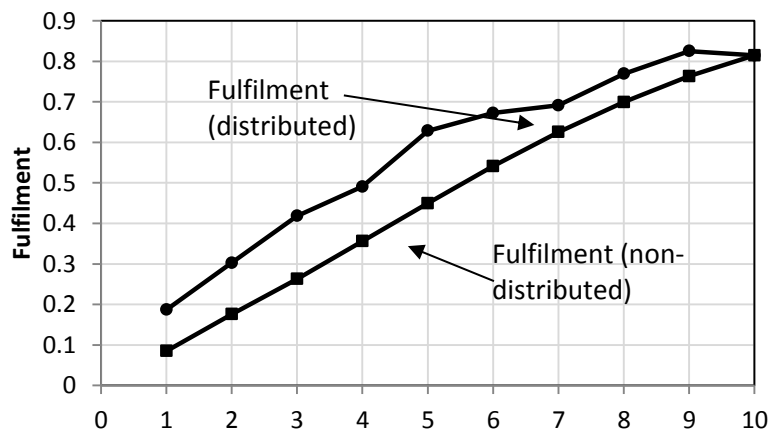


Figure 6.1.2: Implementation Proposal fulfilment coefficient analysis

Curtailment

Figure 6.1.3 shows the curtailment coefficient of the system during the capacity uptake increase and illustrates that the system performs better when the capacity uptake is distributed. During the initial plant implementation of the distributed CSP, the CSP system curtailment was higher than the second capacity uptake. This can be overcome by optimising the CSP to obtain adequate parameters. However, for this study, these parameters were constrained by the fact that the LCOE was optimised for the whole proposed CSP system.

The curtailment energy is the energy that is collected by the solar field but could not be utilised. If the TES is fully charged and thus ready for the peak period, it is possible that this excess energy can be sent to the grid during off-peak period.

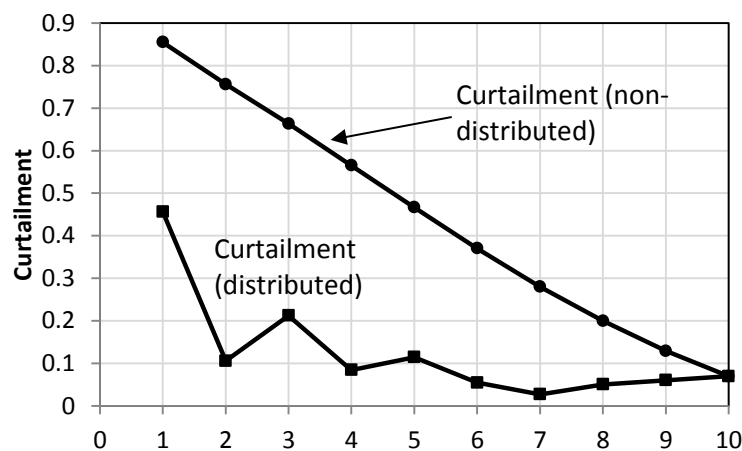


Figure 6.1.3: Implementation proposal curtailment coefficient analysis

6.2 Power Plants Locations

The potential power plant sites are located along the high voltage line that runs towards Cape Town from Gauteng province, as shown in Figure 6.3.1. These potential sites indicate the geographical position of which the DNI solar resource has been extracted and utilized for the modelling in this study. One of the aspects of the development of the CSP plants is the study on land availability. The following section covers the GIS study which gives a brief analysis about the availability of land along this high voltage line.

6.3 GIS Study of Land Availability

The study of land availability for the CSP plants in South Africa has been conducted before by various authors. The first study, conducted by Fluri (2009), investigates the potential of CSP in South Africa. Fluri (2009) considers land availability with a slope of 1 ° or less as well as land that is not further than 20 km from the transmission lines.

The second study was conducted by Meyer & van Niekerk (2012) and provides a roadmap for the development of CSP in South Africa. In this report, land availability for CSP plant development is investigated; it considered land with a 2 ° slope or less that is less than 30 km from the transmission substations.

The construction and development of any power plant requires proper consideration of the challenges of feeding the energy into the grid. According to Meyer & van Niekerk (2012), this unavailability of feed-in substations in close proximity can not only increase project costs but increase project time. The project time can be increased by about 5 years due to development of the needed infrastructure (Meyer & van Niekerk 2012). These findings and observations informed the choice of potential sites for this analysis. Also, the assumption is that the high voltage line has adequate available feed-in capacity. The generated energy from the potential sites will be sent to existing transmission substations. Preferably, this land is also flat or with minimal slope. However, the CSP developers consider land with a 3 ° slope suitable for the development of the central receiver systems. For this study, the GIS software, ArcGIS_ESRI, was used to determine the availability of land around the proposed sites. The Shuttle Radar Topography Mission (SRTM) 90 m digital elevation model (DEM) with a 90 m spatial resolution was utilized to obtain the slope of suitable sites.

Short-term

The ten sites were equally spaced along the high voltage line. Figure 6.3.1 indicates the suitable land for the proposed sites along with the transmission lines and transmission substations. The land that was considered was 30 km in radius or less from the existing transmission substations along the transmission lines and has a slope of 2 ° or less. As previously mentioned, land with up to a 3 ° slope is suitable for CSP plants.

Long-term

The assumption in this long-term study was that the grid infrastructure along the high capacity line was conducive for feeding energy into it. Figure E1 in the Appendix E shows the land availability study that considers the land along the high capacity line. The study considered areas with a slope of 2 ° or less and is 30 km or less from the high voltage line. The land availability analysis can be done by considering many extensions. The long-term analysis shows an example of the long-term potential. The considered transmission line is generally orthogonal to large storms which appear to make the distributed system work better. Initial analysis does not show that there are any exclusion zones along this transmission line. Also, this transmission line is a high capacity line.

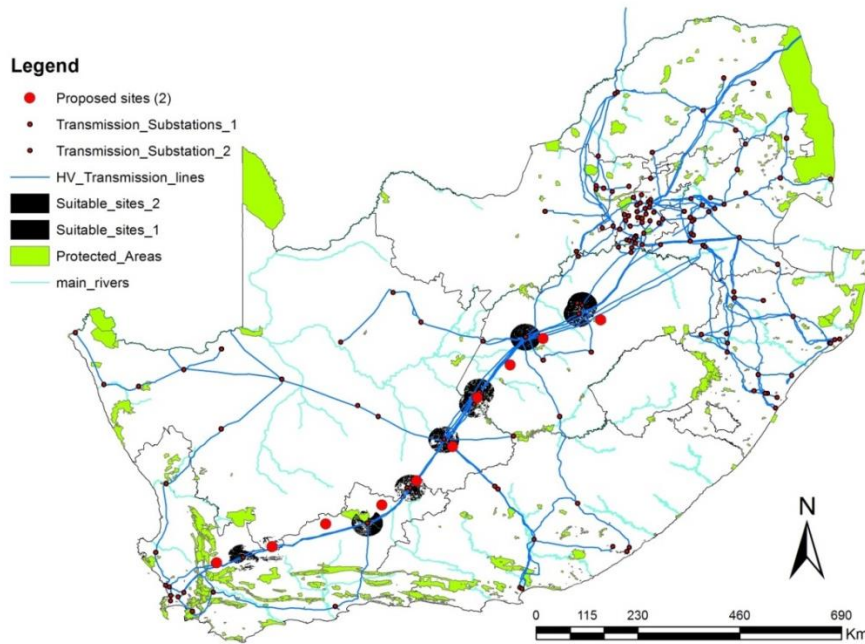


Figure 6.3.1: Land availability along the proposed sites (short-term)

6.4 Conclusion

This chapter presented the proposed the implementation proposal of the proposed CSP system. LCOE, fulfilment and the curtailment of the CSP system were used to analyse the viability of the implementation proposal. The LCOE analysis shows that the distributed CSP system seems to perform better than the non-distributed system. Also, the fulfilment and curtailment from the CSP system seems to perform better when the system is distributed during the phasing implementation. This analysis shows that it is better to distribute the CSP plants during implementation. The land availability analysis shows that there may be available adequate land to implement the proposed CSP system.

7 Conclusions and Further Work

Feasibility of peaking CSP systems in SA is conducted in this study. The literature survey conducted showed the current state and future state of electricity industry in South Africa. By reviewing the IRP, the literature survey showed that the capacity allocation to CSP is minimal. The literature concluded by looking at the work that has been done on other studies to illustrate the dispatch potential of CSP technology. This work showed that there is a potential of utilising CSP systems as peaking systems.

Three scenarios of the peaking systems in SA have been developed and presented. The OCGT system scenario shows that these systems generate energy in excess of 5.08 ZAR/kWh. Furthermore, this scenario shows that the OCGT systems are vulnerable to fluctuating diesel prices. The CSP scenario established that the CSP systems generate the peak energy at 1.89 ZAR/kWh. The utilization of grid electricity by CSP systems to supply the gap energy demand results in LCOE increase of 37 %. LCOE increases from 1.89 ZAR/kWh to 3.00 ZAR/kWh. This is still financially better than the OCGT LCOE. The scenario that combines the CSP system and the OCGT system as a virtual hybrid system results in a combined LCOE of 2.78 ZAR/kWh. This scenario results in the lowest LCOE and guarantees electricity generation.

The two scenarios that were developed and compared to the OCGT scenario show that that the CSP performs well as peaking system in South Africa. Also, it results in lower LCOE than the OCGT system. The scenario that seems to perform well and guarantee energy supply is the virtual hybrid systems scenario. The consequence of the combined system is that SA does not need to gratuitously invest in CSP. A fleet of CSP plants optimized to be used with the OCGT fleet appear to drop the net cost of electricity while showing impressive resilience to fuel price fluctuations. This scenario allows the energy industry to add 3 300 MW of CSP into the grid without a subsidy.

The next proposed step is to optimise the model for phasing implementation. Currently, the CSP model is optimised for the LCOE of the total proposed CSP system capacity. This study revealed that proper distribution of CSP plants during implementation affects the LCOE and that the distributed plants perform better than the non-distributed plants. Assumptions were made based on the fact that actual recorded data from the Gemasolar plant were not available during the development of the model; these assumptions involved the storage charge efficiency, storage thermal loss efficiency and parasitic power consumption etc. The model used conservative assumptions in this regard. In future, it would be important to obtain actual numbers from the Gemasolar plant.

8 References

Black and Veatch. 2012. Cost and performance data for power generation technologies. Prepared for the National Renewable Energy Laboratory.

Brinckerhoff, P. 2008. Cost estimates for thermal peaking plant – final report. Parsons Brinckerhoff New Zealand Ltd.

Brinckerhoff, P. 2011. Electricity generation cost model – 2011 update revision 1. prepared for Department of Energy and climate change.

Creamer, T. 2013. Long-delayed peaker projects to reach financial close “next week”. Engineering News online, Creamer media, [Online]. Available: www.engineeringnews.co.za/print-version/long-delayed-peaker-projects-to-reach-financial-close-next-week. [09 May 2013].

Creamer, T. 2013a. South Africa aims to finalise Integrated Energy Plan in 2014. Engineering News online, Creamer media. [Online]. Available: <http://www.engineeringnews.co.za/article/south-africa-aims-to-finalise-integrated-energy-plan-in-2014>. [25 October 2013].

Creamer, T. 2013b. Surging tariffs and interest bill, but also signs of greater stability at Eskom. Engineering News online, Creamer media, [Online]. Available: <http://www.engineeringnews.co.za/article/eskoms-interest-bill-surging-but-funding-plan-advanced-2011-07-08>. [14 May 2013].

Crespo, L., Dobrotkova, Z., Philibert, C., Richter, C., Simbolotti, G. and Turchi, C. 2012. Renewable energy technologies: cost analysis series. concentrating solar power. The International Renewable Energy Agency (IRENA).

Denholm, P., Wan, Y., Hummon, M. and Mehos, M. 2013. An analysis of concentrating solar power with thermal energy storage in a California 33 % renewable scenario. National Renewable Energy Laboratory (NREL).

Denholm, P. & Mehos, M. 2011. Enabling greater penetration of solar power via the use of CSP with thermal energy storage. National Renewable Energy Laboratory (NREL).

DoE, 2013a. Draft 2012 Integrated Energy Planning Report, Executive Summary. Department of Energy.

DoE, 2013b. Draft Integrated Energy Planning Report, Presentation to portfolio committee on energy. Department of Energy.

DoE, 2011. Integrated Resource Plan for Electricity 2010 - 2030. Revision 2, final report. Department of Energy.

References

DST, 2009. Karoo Astronomy Geographic Advantage Act. Act No. 21 of 2007 Government Gazette. Department of Science and technology. published in the Government Gazette, volume 516, Cape Town, 17 June 2008, [Online]. Available: www.dst.gov.za/publications-policies/legislation/Astronomy%20Geographic%20Advantage%20Act.pdf

Eskom. 2009. Ankerlig and Gourikwa gas turbine power stations, facts sheet. produced by: generation communication/ group communication GS 0002 revision 5 (June 2010). (www.eskom.co.za). select the “knowledge centre” and “facts and figures”

Eskom. 2010. Ankerlig and Gourikwa gas turbine power stations, facts sheet. produced by: generation communication/ group communication GS 0003 revision 1 (January 2009). (www.eskom.co.za). select the “knowledge centre” and “facts and figures

Eskom, 2010b. Generation connection capacity assessment of the 2012 transmission network (GCCA-2012). Eskom.

Eskom, 2012a. Integrated Report for the year ended 31 March 2012. Eskom.

Eskom, 2012b. tariffs & charges booklet for the year 2012/2013. Eskom

Eskom, 2012c. Transmission ten-year development plan 2012-2021. Eskom transmission division. Eskom.

Fluri, T. 2009. The potential of concentrating solar power in South Africa. Energy Policy, Volume 37(12), pp.5075–5080.

Gary, J., Turchi, C. and Siegel, N. 2011 CSP and the DoE SUNSHOT initiative. U.S. Department of Energy, solar energy technologies program. National Renewable Energy Laboratory. Sandia National Laboratories.

Gauché, P., Pfenninger, S., Meyer, A. and Brent, A. 2012. Modeling dispatchability potential of CSP in South Africa. SASEC 2012. May 2012.

Gauché, P., von Backström, T. and Brent, A.C. 2012. A value proposition of CSP for South Africa. SASEC 2012. May 2012.

Gauché, P., von Backström, T. and Brent, A.C., 2011. Modelling methodology for macro decision making – emphasis on the central receiver type, SolarPACES conference, concentrating solar power and chemical energy systems, Granada, Spain, September 20-23, 2011.

References

Gonzalez, B. 2013. BBenergy solar based energy project at Rosherville exceeds design expectations. CSP Today. [Online]. Available: (<http://social.csptoday.com>) [03 June 2013].

Häberle, A., Zahler, C., Lerchenmüller, H., Mertins, M., Wittwer, C., Trieb, F. and Dersch, J. s.a. The Solarmundo line focussing Fresnel collector . optical and thermal performance and cost calculations. Fraunhofer Institute for Solar Energy Systems. German Aerospace Center (DLR) - Institute of Technical Thermodynamics. German Aerospace Center (DLR) - Institute of Technical Thermodynamics-Solar Research

Hartnady, C.J.H. 2010. South Africa's diminishing coal reserves, South African Journal of Science, Vol. 106, Art. 369.

Heap, B. 2011. Concentrating solar power: its potential contribution to a sustainable energy future. European Academies of Science Advisory Council (EASAC). EASAC policy report 16. November 2011.

Helman, U. 2012. Valuing concentrating solar power with thermal energy storage. Presentation at the California Energy Commission Staff Workshop. Solar Thermal Energy Storage and Solar Cogeneration Sacramento, California. August 2012.

Helman, U. & Kroyzer, O. 2006. Valuing thermal energy storage in CSP systems. BrightSource Energy Inc.

International energy Agency (IEA). 2010. Technology Roadmap Concentrating Solar Power, IEA, 2010.

Kolb, G., Ho, C. K., Mancini, T. and Jesse, A.G. 2011. Power Tower Technology Roadmap and Cost Reduction Plan. Sandia National Laboratories. Sandia Report. SAND2011-2419 Unlimited Release Printed April 2011.

Kost, C. D. R., Schegl, T., Thomsen, J. and Nold, S. 2012. Levelized cost of electricity renewable energies. renewable energy innovation policy Fraunhofer Institute for Solar Energy Systems ISE. Fraunhofer. May 2012.

Lata, J.M., Rodriguez, M. and Alvarez de Lara, M. 2008. High flux central receivers of molten salts for the new generation of commercial stand-alone solar power plants. Journal of Solar Energy Engineering. Vol. 130 / 021002-1. May 2008.

Lubkoll, M. 2011. A pre-feasibility study of a concentrating solar power system to offset electricity consumption at the Spier Estate. Master Thesis. Stellenbosch University.

References

- MAE. 2013. Thermodynamics Lecture. West Virginia University – Mechanical and Aerospace Engineering [Online]. Available: <http://www.mae.wvu.edu/~smirnov/mae320/notes.html> [08 October 2013]
- Mail and Guadian (M&G). 2013. Koeberg electric fault leaves Eskom on tight margin. [Online]. Available: <http://mg.co.za/article/2013-02-21-koeberg-at-half-capacity> [14 May 2013]
- Mail and Guadian (M&G), 2013b. Nersa gives Eskom annual 8 % tariff increase. [Online]. Available: <http://mg.co.za/article/2013-02-28-nersa-rejects-eskoms-16-tariff-bid> [14 May 2013]
- Madaeni, S.H., Sioshansi, R. & Denholm, P. 2011. Capacity value of concentrating solar power plants capacity value of concentrating solar power plants. National Renewable Energy Laboratory. technical report NREL/TP-6A20-51253 June 2011.
- Meyer, A.J. 2012. The South African REFIT: Solar resource assessment options for solar developers. SASEC. May 2012.
- Meyer, A.J. & van Niekerk, J.L. 2012. Roadmap for the development of concentrating solar power in South Africa. SolarPACES conference, concentrating solar power and chemical energy systems, Granada, Spain, September 20-23, 2011.
- Moolman, S. 2013. Plans a foot to increase the role of gas in SA 's energy mix. Engineering News online, Creamer media. [Online]. Available: www.engineeringnews.co.za/print-version/plans-afoot-to-increase-the-role-of-gas-in-sas-energy-mix [21 June 2013].
- National Renewable Energy Laboratory (NREL). 2011. Gemasolar thermosolar plant project overview, NREL/SolarPACES, [Online]. Available: http://www.nrel.gov/csp/solarpaces/project_detail.cfm/projectID=40, accessed 20 May 2013.
- Novikov, I.I. 1957. The Efficiency of atomic power stations. Journal Nuclear Energy II, 7:125–128, 1958. Translated from Atomnaya Energiya, 3 (1957), 409.
- Ogbonnaya, E.A. 2004. Active condition monitoring of a marine gas turbine through rotor shaft vibration analysis. American Journal of Mechanical Engineering. Volume 4, pp. 82-88.
- Pacheco, J.E. 2002. Final test and evaluation results from the Solar Two project. solar thermal technology, Sandia National Laboratories. SAND2002-0120 unlimited release.

References

Patzek, T.W. & Croft, G.D. 2010. A global coal production forecast with multi-Hubbert cycle analysis. *Energy*, Volume 35, pp.3109–3122.

Pitz-Paal, P.D. 2012. Concentrating Solar Power - A Roadmap from research to market. presentation. Institute of Technical Thermodynamics Solar Research German Aerospace Centre (DLR).

REIPPPP, 2013. Department of Energy, Renewable Energy IPP Procurement Programme. Bid Window 3 Preferred Bidders's announcement. 4 November 2013.

Rutledge, D. 2011. Estimating Long-term world coal production with logit and probit transforms. *International Journal of Coal Geology*, volume 85(2011), pp.23–33.

Sener, 2010. Case Study: GEMASOLAR central tower plant. *CSP Today*, San Fransisco. 24 & 25 June 2010.

Siemens, 2012. The SGT-2000E series – designed for reliable, robust, and flexible power generation. Siemens Gas Turbine. SGT – 2000E series. 2012

Sioshansi, R. & Denholm, P. 2010. The value of concentrating solar power and thermal energy storage. National Renewable Energy Laboratory (NREL). Technical Report NREL-TP-6A2-45833. February 2010.

SolarPACES, 2012a. CSP how it works. Technology characterization solar dish systems. [Online]. Available: http://www.solarpaces.org/CSP_Technology/csp_technology.htm. accessed 30 May 2013.

SolarPACES, 2012b. CSP how it works. Technology characterization parabolic trough system. [Online]. Available: http://www.solarpaces.org/CSP_Technology/csp_technology.htm. accessed 30 May 2013.

SolarPACES, 2012c. CSP how it works. Technology characterization solar power tower system. [Online]. Available: http://www.solarpaces.org/CSP_Technology/csp_technology.htm. accessed 30 May 2013.

Stine, W.B. & Geyer, M. 2001. Power from the Sun. Power from the Sun.net. J.T Lyle Center for Regenerative Studies. 2001.

Torresol Energy. 2013. Gemasolar themorsolar plant pictures. Torresol Energy. <http://www.torresolenergy.com/TORRESOL/gemasolar-plant/en> [08 October 2013]

References

USDoE. 2011. U.S Department of Energy, energy efficiency & renewable energy. 2010 Solar technologies market report. November 2011.

US DoE. 2013. Concentrating solar power basics. US Department of Energy. [Online]. Available: <http://energy.gov/eere/energybasics/articles/linear-concentrator-system-basics-concentrating-solar-power> [08 October 2013]

APPENDIX A – ZENITH ANGLE CALCULATION

Figure A.1 shows the sun angles relative to the heliostat. The solar field operational parameters in Chapter 1 Technical Model Development stated that the optical performance of a solar field is dominated by the zenith angle. This section discusses how the Zenith angle calculated.

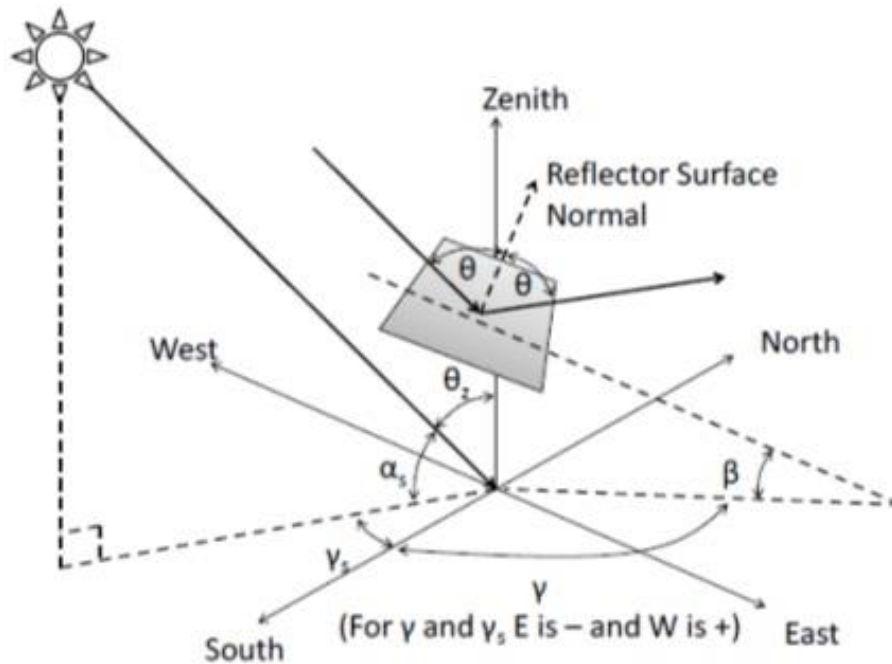


Figure A1: Sun angles relative to the heliostat spectrum (Stine & Geyer 2001)

The equation below is used to determine the Zenith angle:

$$\cos \theta_z = \cos \varphi * \cos \delta * \cos \omega + \sin \varphi * \sin \delta \quad (\text{A.1})$$

| | |
|------------|-------------------|
| θ_z | Zenith angle |
| φ | Latitude |
| δ | Declination angle |
| ω | Hour angle |

The declination angle (δ) – the angle of zenith relative to the equator due to the tilted rotation axis of earth is derived by the following formula:

$$\delta = 0.006918 - 0.399912 \cos B + 0.070257 \sin B - 0.006758 \cos 2B + 0.000907 \sin 2B - 0.02679 \cos 3B + 0.00148 \sin 3B \quad (\text{A.2})$$

Hour angle (ω) – is the conversion of solar time to an angle where 24 hours = 360° and solar noon is zero. It is derived by the following equation:

$$\text{Hour angle} = (\text{solar time} - 12) * 15 \quad (\text{A.3})$$

Solar time – is the time reference and is defined by solar noon, the time when the sun crosses the meridian of the observer.

$$\text{Solar time} = \text{standard time} + 4(\text{local standard time} - \text{longitude}) + \text{Equation of time} \quad (\text{A.4})$$

$$\text{Equation of time (E)} = 9.2 (0.000075 + 0.001868 \cos B - 0.032077 \sin B - 0.014615 \cos 2B - 0.04089 \sin 2B) \quad (\text{A.5})$$

B converts the day of the year to an angular value for the trigonometry.

$$B = \frac{(\text{year day} - 1) * 360}{365} \quad (\text{A.6})$$

APPENDIX B – POWER PLANT SCALING

This section illustrates the scaling of the three independent yet interrelated primary components.

- The solar field, which collects the solar radiation and produces the thermal energy.
- The TES system, which stores the thermal energy in the HTF.
- The turbine, which converts the thermal energy and mechanically transfers that energy into the electricity generator.

Figure B.1 shows the configuration of the above mentioned CSP components.

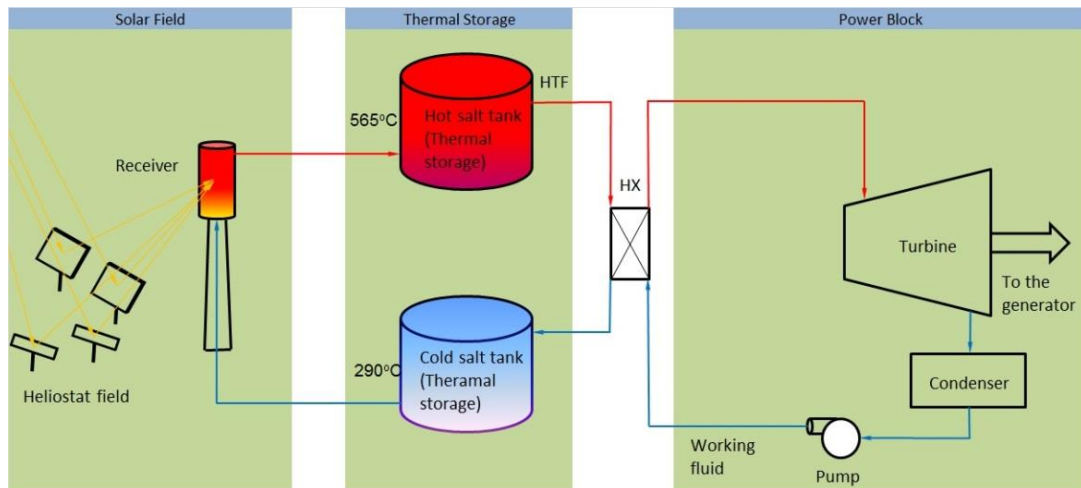


Figure B.1: CSP primary components

The specified component sizes and operating parameters for the Gemasolar plant are 20 MW turbine with 15 hours storage TES and a solar field. In order to achieve the adequate capacity that meets the assumed peak load demand, these parameters were scaled up or down.

Scaling of these components is illustrated in Figure B.2 and Figure B.3. The capacity of each component can form a single primary component – one single solar field or it can be from smaller sized solar field with the equal combined capacity. The scaling ratio is maintained for the TES and the Turbine. The TES proposed capacity can be from a single TES system or it can be from a number of smaller TES systems with the equal combined capacity.

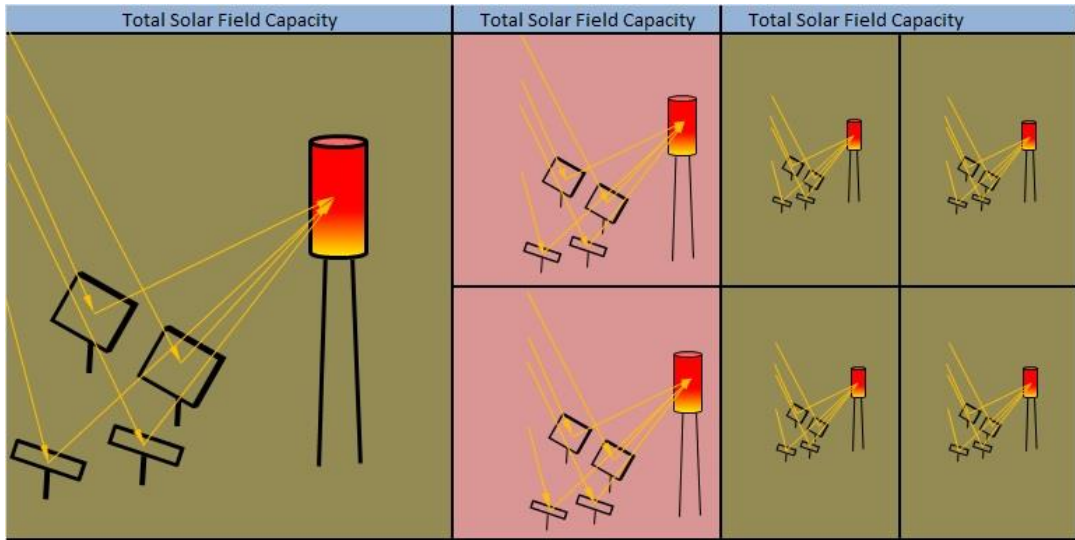


Figure B.2: Solar field and tower scaling

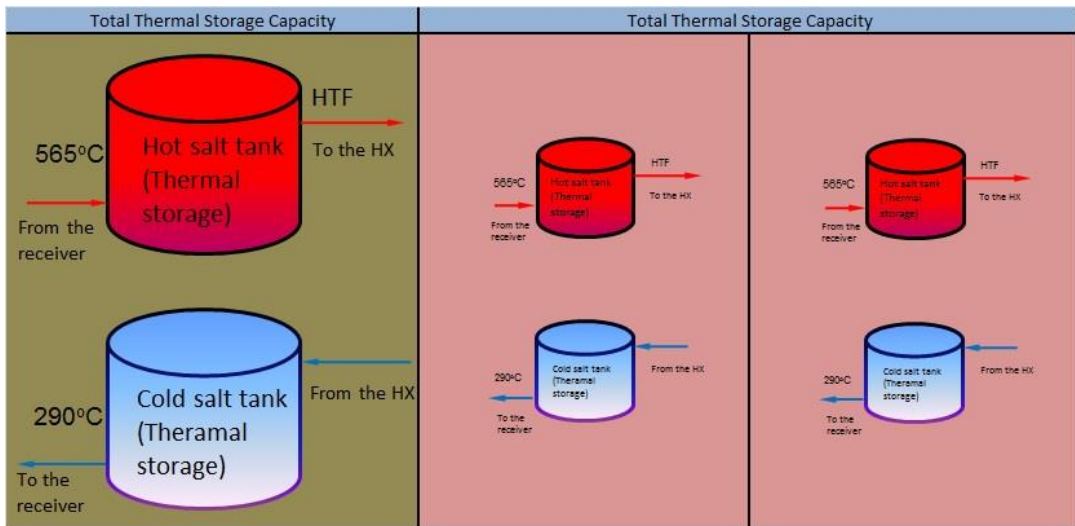


Figure B.3: TES scaling

APPENDIX C – CURTAILMENT

Figure C.1 shows the storage charge level and the curtailment energy for three days for the total TES system from all sites.

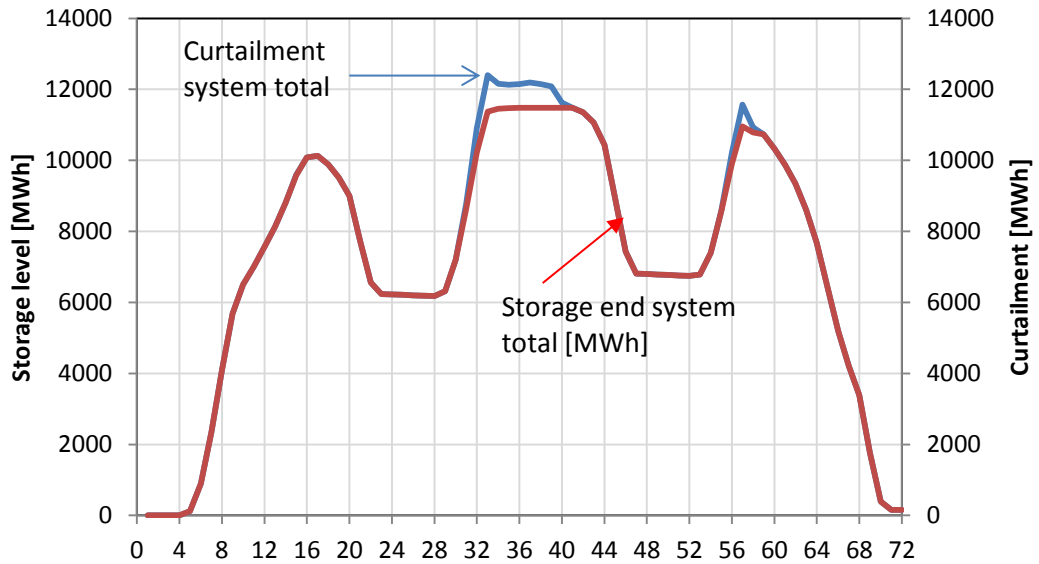


Figure C.1: Storage charge level and energy curtailment – total system

APPENDIX D – COMPARISON OF ACTUAL DNI VS PREDICTED DNI

The Figure D.1 shows the actual DNI and the predicted DNI. The values are derived from site 1 DNI for January.

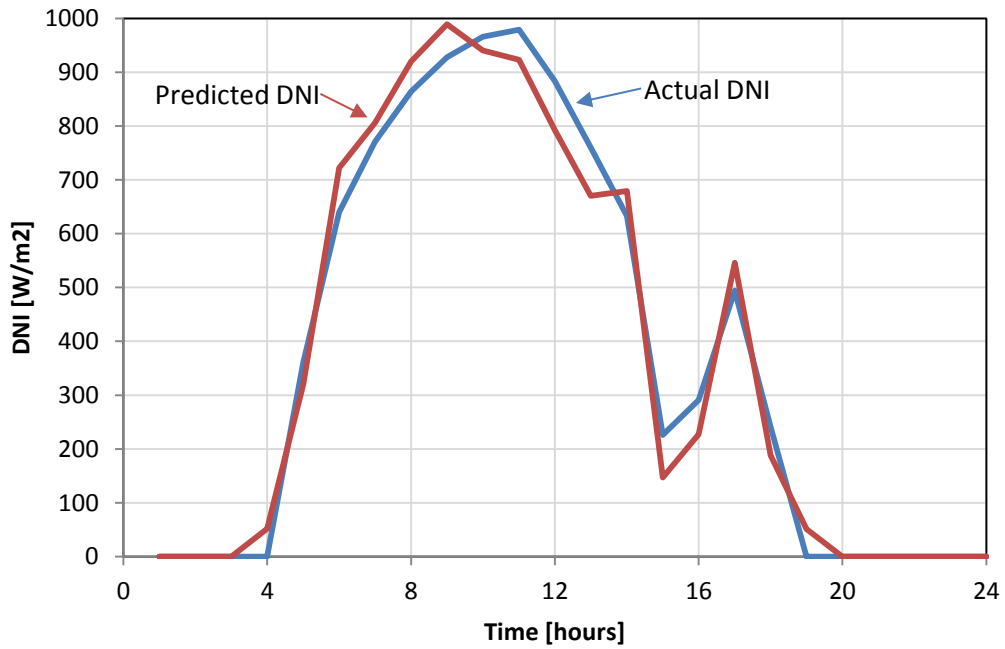


Figure D1: Actual DNI vs predicted DNI

APPENDIX E – POWER PLANTS LOCATIONS

Figure E.1 indicates the suitable land for the proposed sites along with the transmission lines and transmission substations. The land that was considered was 30 km or less from the existing transmission substations along the transmission lines and has a slope of 2 ° or less.

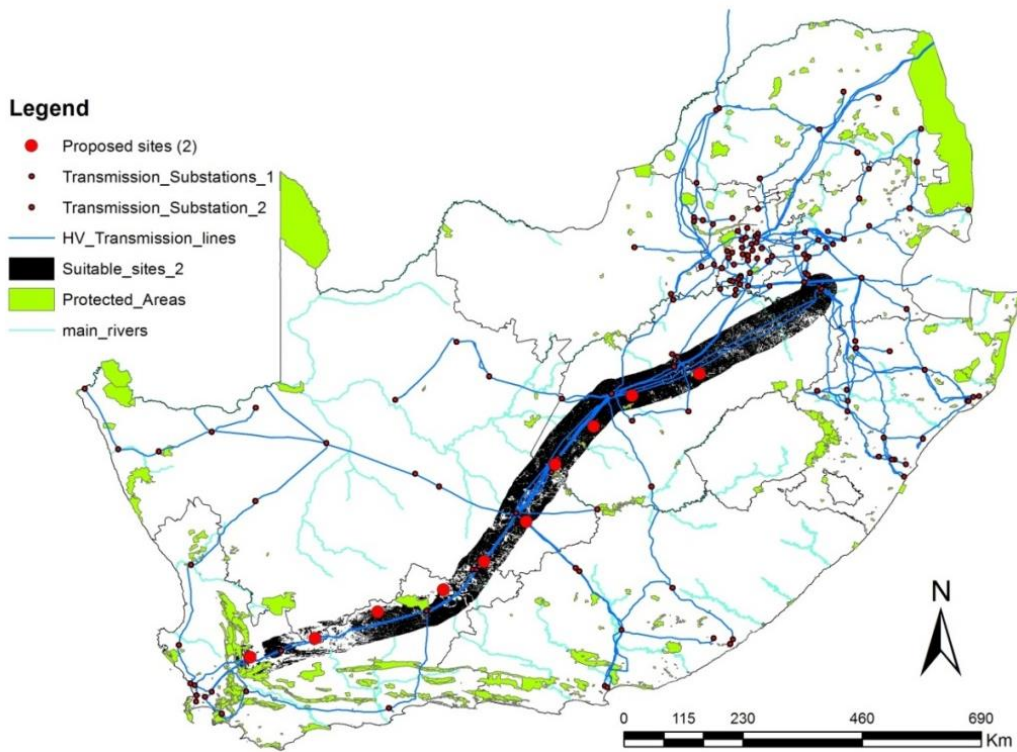


Figure E1: Land availability along the proposed sites (long-term)